Robot Simultaneous Localisation and Mapping with Dynamic Objects

Yash Vyas
U5388842

Supervised by Dr. Viorela Ila and Dr. Jochen Trumpf

October 2017

A thesis submitted in part fulfilment of the degree of

Bachelor of Engineering
The Department of Engineering
Australian National University

This thesis contains no material which has been accepted for the award of any other degree or diploma in any university. To the best of the author's knowledge, it contains no material previously published or written by another person, except where due reference is made in the text.

Yash Vyas
27 October 2017

Acknowledgements

Thank you to Dr. Viorela Ila and Dr. Jochen Trumpf, for being extremely helpful supervisors who constantly challenged me and guided me towards improving myself. I would also like to thank Mina Henein, Montiel Abello and Professor Rob Mahony for providing additional guidance in understanding this subject.

Completing this project would not have been possible without my mother Gaurangi Vyas, whose constant care enabled me to complete this honours project with all of my other coursework, and my friends who were always there to support me when needed.

Abstract

This honours project develops a framework to integrate dynamic motion information in a Simultaneous Localisation and Mapping (SLAM) algorithm. The purpose of the framework is to track moving objects in a robot's environment and integrate their motion information in a SLAM algorithm. Our expectation is that integrating the motion information of objects in a robot's environment increases the SLAM solution accuracy.

The framework has a front end that can generate simulated data with motion information according to several types of motion models, and a back end that processes the data through our SLAM solver algorithm to produce the final estimate. I contributed to the development of the front-end, and used the framework to test the validity, accuracy, and improvement in the SLAM estimation of these motion models.

The results show that integrating the motion estimation of objects in a robot's environment improves the estimation accuracy of the constructed map and robot's position within it, however only for cases where the motion model used by the solver is an accurate representation of the actual motion. The most robust and realistic motion estimation from the models tested is constant motion. Tests on the algorithm with the constant motion estimation showed that it consistently improves the SLAM final estimate of the robot's localisation and map.

Contents

List of Figures

List of Tables

Glossary of Terms

ACRV	Australian Centre for Robotic Vision
DOF	Degree of Freedom
DO-SLAM	Dynamic Object Simultaneous Localisation and Mapping
IMU	Inertial Measurement Unit
LIDAR	Light Detection and Ranging
NLS	Non-Linear Least Squares
OOP	Object Oriented Programming
RGB	Red-Green-Blue
SLAM	Simultaneous Localisation and Mapping

Chapter 1

Introduction

1.1 Context

Autonomous machines and devices have become ubiquitous in the past few decades, leading to increases in productivity and the capability to execute high precision and specialised application tasks. Robots in particular have been extensively developed to replace previously human-controlled functions ranging from cleaning to aerial imaging and surveying. Robotic devices typically utilise a multiple types of sensors such as inertial measurement units (IMU), RGB cameras, depth cameras, ultrasound, LIDAR, and many others. The sensors gather data on the environment which a microcontroller processes to obtain information needed to perform higher level tasks, for example feedback and control of actuators, navigation, and path planning, which are required for the robot to fulfil its application.

For mobile robots, knowledge of the robot's environment and its location within it is required for operational tasks such as navigation, path planning and steering. To operate in an unknown environment, a robot needs to incrementally build a map of their environment while localising itself within that map. This problem is known in the robotics field as Simultaneous Localisation and Mapping (SLAM) [3].

Detailed information about a robot's environment (e.g. structure, appearance and position of objects such as buildings) can be acquired from robot sensor data and used to accurately model the real world, which in the computer vision field is referred to as Structure from Motion (SfM) or 3D reconstruction. Improving the map estimate also involves improving the robot localisation, therefore both SLAM and SfM are essentially the same problem: that of creating an abstract representation of an environment while also localising the sensors that obtained the environment data. Currently, SLAM is extensively used in Virtual and Augmented Reality applications in devices such as the Microsoft HoloLens and Google Pixel.

Robots are increasingly being deployed in cluttered environments where the majority of objects that can be sensed are dynamic, not static. Dynamic is defined here as having motion, so that the position and orientation of the object can change with time. Current state of the art SLAM applications are predominantly designed to work in static environments, and employ a static assumption of features tracked

in the environment while the robot moves. Some SLAM implementations estimate whether a tracked feature has motion, and rejects the feature from the SLAM solution system as an outlier. However for a highly dynamic environment this reduces the quantity of repeated measurements of tracked features which leads to reduced accuracy of the map and robot localisation estimate.

The Australian Centre for Robotic Vision (ACRV) at the ANU is actively involved in research that fuses advances made in both the computer vision and robotics fields. This project is part of a research program that is researching a framework for dynamic SLAM, where dynamic information of the robot's environment are used in the SLAM algorithm, unlike traditional SLAM implementations that assume static environments.

This framework, known as Dynamic Object SLAM (DO-SLAM) can do the following:

1. Generate data of an simulated environment containing both static and dynamic objects with structure.

2. Process the simulated environment data or real world data through a specialised sensor code to form a SLAM system consisting of the robot trajectory, map objects, and motion/structure information of these objects for solution.

3. Solve this SLAM system for the robot trajectory and map estimate using a square root smoothing and mapping algorithm [4].

Integrating the motion of dynamic objects in the SLAM algorithms is expected to have the following benefits:

1. Increased robustness of the SLAM algorithm in highly dynamic environments.

2. Localisation and tracking of moving objects, which can assist in other high-level robot tasks such as navigation and collision avoidance.

3. Improved accuracy of the SLAM estimation of the robot's trajectory and environment.

Testing the third claim is a main objective of this project, and investigating all three benefits is the objective of the research program I am part of.

1.2 Project Scope

The scope of this project is to develop a simulation framework to test algorithms for SLAM and tracking of dynamic objects. The deliverables include:

1. A front-end simulator which can create an environment consisting of simple primitives with structure and motion behaviour.

2. Sensors that can process simulated or real world data to create measurements of the robot odometry, sensing of objects and their structure/motion, to form a factor graph.

3. Solver implementation that can parse the factor graph and solve for the robot poses and map using non-linear least squares optimisation.

1.3 Thesis Contributions

My contributions towsards the development the DO-SLAM framework are the following:

1. Conceptualisation of the Object Oriented Programming (OOP) framework implementing the method including the simulated environment, sensor types, and SLAM solver, known as Dynamic Object SLAM (DO-SLAM) (section 4.1 and chapter 5).

2. Implementation of this framework in MATLAB, including:

   (a) Development of functionality in the simulated environment to represent structured objects (such as primitives) with points (that abstract tracked features on an object), and motion (subsection 5.1.4).

   (b) Development of a Simulated Environment Sensor that can model occlusion (section 4.4), and create measurements of objects and points with their associated motion measurement or estimations (subsection 5.1.5).

3. Creating testing environments and using them to validate and test the accuracy of motion estimation and constraint models (chapter 6).

4. Contributing to the simulation section of a paper submission to the International Conference of Robotics and Automation 2018 (ICRA'18) [2].

The MATLAB parent class implementation for the front end is due to Montiel Abello, and my work builds on that foundation by writing inheriting classes implementing specific types of trajectories, environment utils and sensors, along with modifications to the original code that adds required functionality.

The graph and solver implementation is based on a previous iteration of the framework known as Dynamic SLAM which is due to Mina Henein and Montiel Abello [5]. Implementation of the measurements and constraints in the graph and

solver back-end classes is due to Mina Henein. The conceptualisation of the overall structure of DO-SLAM and dynamic SLAM methodology is due to Viorela Ila with input and guidance from Jochen Trumpf and Robert Mahony.

1.4 Thesis Structure

This thesis begins with an introduction (chapter 1) which outlines the context for developing a framework to solve SLAM with incorporation of dynamic motion information (DO-SLAM), and briefly summarises its developments and my contributions within the project scope.

Chapter 2 provides a literature review of some of the previous developments in SLAM and in particular, dynamic SLAM that are relevant to the research in this honours thesis.

Chapter 3 is the background theory, which describes some of the common geometric representations used in the robotics field to represent positions and poses in 3-D space, and the general SLAM problem formulation as a joint probability, factor graph and non-linear least squares problem.

Chapter 4 on method has a detailed conceptual explanation of the design of DO-SLAM framework and how it abstracts of environment information, and formulates it as a SLAM problem by incorporation of motion measurements and constraints.

Chapter 5 on implementation provides a description of the OOP aspects of the DO-SLAM framework's code structure and functionality.

Chapter 6 contains the results of the applications used to test the SLAM algorithms, including details on the experimental setup and an evaluation of the performance of different motion models with respect to chosen error measures.

Chapter 7 is the conclusion which summarises the key findings from this honours research project and future work in this subject.

Chapter 2

Literature Review

2.1 Previous Work in SLAM

Two approaches developed to solve the SLAM problem are filtering and global optimisation. Both methods use model the robot state(s), environment, and measurements as probabilities. Filtering methods use the current and previous time step for estimation, thereby previous states of the robot and map are not stored and used. The Extended Kalman Filter (EKF) is the most common method of solving standard SLAM problems, which contains the robot pose at the current time step and all of the detected landmarks in the environment [3]. EKF estimation requires that non-linear state transition and measurement models have to be linearised around the current estimate values, which over time results in increasing error in the robot and map estimation. Furthermore, the EKF matrices are dense and computation time for the matrix operations in the filter update increases significantly as the size of the map grows [4].

On the other hand, global optimisation methods for SLAM use the entire robot trajectory up to the current time in its solution, and minimise the error for joint probability of all the robot poses and sensor measurements. In linear algebra based global optimisation, a non-linear least squares problem is formed from the measurements of the entire robot trajectory and the map, and the linearisation points of the system are recalculated for each iteration of the solution algorithm which avoids the error accumulated by locking them at every time step. Non-linear least squares matrices also have the advantage of having sparser matrix structures than filters, which reduces computation time for large systems. The DO-SLAM framework solver uses a global optimisation algorithm known as Square Root Smoothing and Mapping [4], which is explained in detail in section 3.2.

The multiple robot problem is the converse to dynamic SLAM it tracks landmarks in the environment over multiple moving robots rather than tracking multiple moving objects from a single robot. DDF-SAM is a method of solving the multiple-robot problem by fusing distributed data from multiple robots to build a decentralised and concurrent map of the environment [6, 7]. Factors are shared between robots to form a consistent neighbourhood graph that finds the joint probability

estimate for all of the measurements taken from the different robots. The system is incrementally solved for the robot and neighbourhood graphs, with only information of relevant landmark variables passed between both graphs (factor graphs are explained in subsection 3.2.2). Although this problem tracks landmarks observed by multiple dynamic robots, it does not use the augmented neighbourhood graph to improve estimation of the robot trajectories, therefore there are the DDF-SAM algorithm does not have any significant aspects that can be adapted to DO-SLAM.

Grouping points in the scene with structure is an important aspect of estimating rigid body motion for objects in an environnment. SLAM++ is an algorithm to solve SLAM problems in structured indoor environments containing repetitive objects [8]. Its approach is to detect and associate object features with an internal 6-DOF representation of object structure, which allows for a more compact representation and additional structural information which improves the map estimate. In DO-SLAM we assume that the point-object data association problem has been solved and directly calculate the motion of points on moving objects, however the ability to estimate the pose of a rigid body through fitting structure to points can help us adapt our algorithm for other motion models apart from constant motion.

2.2 Dynamic SLAM

Dynamic changes to a robot's environment can be classified into two types: long-term and short-term. Long-term changes imply that the landmarks in a robot's environment can be assumed to be static compared to the speed of the robot. Short-term dynamic changes imply that the landmarks' velocity is at the same order of magnitude as the robot, so its motion must be accounted for during the robot's sensor data collection and the map estimation.

The authors in [9] develop a method to distinguish long-term dynamic changes in an environment as part of the map estimation. The research uses pose-graph optimisation techniques (Dynamic Pose Graph SLAM) to solve for the static and moving landmarks between separate passes of the environment in order to maintain an efficient and up-to-date map.

SLAMIDE [10] is an algorithm that distinguishes between dynamic and static landmarks in an environment for short-term dynamic changes. It does this by implementing reversible model selection and reversible data association, done by a generalised expectation maximisation algorithm on the state information matrix for a sliding window of previous time steps. Both dynamic motion information and static measurements can be incorporated in the same Bayesian network with data association that differentiates between static and dynamic landmarks and applies

appropriate motion models in the SLAM solver.

Distinguishing between static and moving objects is assumed to be solved in the current state DO-SLAM solver, and both approaches in [9] and [10] could be incorporated in our framework to make our algorithm more robust in real world environments. SLAMIDE is more suitable as it estimates the motion behaviour of landmarks simultaneously with the robot pose estimation, which is more suited for estimating short-term dynamic changes.

SLAMMOT [11] is a framework that includes tracking of moving objects in a scene. The authors present two approaches: the first approach modifies the generalised SLAM algorithm to model and solve the motion of all objects in the scene together, however the researchers claim this is computationally infeasible. The second version separates the estimation of static and dynamic objects into two separate estimators, which reduces the dimensionality of the SLAM system. SLAMMOT is similar to DO-SLAM in that it integrates object tracking and motion estimation for dynamic objects in the SLAM algorithm. However, DO-SLAM solves for both static and dynamic objects in the same solver in a computationally feasible way.

Chapter 3

Background Theory

3.1 Geometric Representations

3.1.1 Position

The map is defined as the abstract representation of the robot environment. It consists of points that represent features in the environment that can be tracked by a sensor, and objects that groups points together with structure. Points and objects exist spatially with respect to an inertial frame. Geometric representations are used to quantify the properties of objects and associated points in the map.

The map in this framework is a 3-dimensional Euclidean geometry space. The most utilised geometric representation of position in this space is $\mathbb{R}^3$ rectangular coordinates x,y and z:

$$\mathbf{t} = \begin{bmatrix} x \\ y \\ z \end{bmatrix} \tag{3.1}$$

An alternate representation of this coordinate space is using spherical coordinates, which treats the position of a point as lying along the surface of a spheroid centred on the reference frame origin, with coordinates radius, azimuth and elevation. The radius r is the euclidean distance of the position in $\mathbb{R}^3$ from the origin of the reference frame. To find the azimuth and elevation, we find the ray vector between the position's $\mathbb{R}^3$ coordinates and the origin. The azimuth θ is the anti-clockwise angle of that ray in the x-y plane from the positive x-axis. The elevation ϕ is the angle between that ray and x-y plane. The conversion between $\mathbb{R}^3$ and spherical coordinates is (3.2), illustrated in Figure 3.1.

$$\begin{bmatrix} r \\ \theta \\ \phi \end{bmatrix} = f(\mathbf{t}) \begin{bmatrix} \sqrt{x^2+y^2+z^2} \\ \arctan(\frac{y}{x}) \\ \arctan(\frac{z}{x^2+y^2}) \end{bmatrix} \tag{3.2}$$

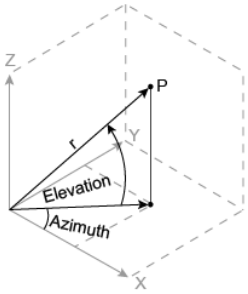

Figure 3.1: Graphical explanation of position as expressed in spherical coordinates. Source: [1]

3.1.2 Rotation Matrices

For any position represented using $\mathbb{R}^3$ a 3×3 transformation matrix $\mathbf{R}$ maps between any two elements in $\mathbb{R}^3$, $\mathbf{t_1}$ and $\mathbf{t_2}$:

$$\mathbf{t_2} = \mathbf{R}\mathbf{t_1} \tag{3.3}$$

The set of all invertible matrices forms the General Linear Group, and can rotate, reflect, and skew a point about the reference frame origin. Within this group, the set of orthogonal matrices form the Orthogonal Group O(3). These have the following properties [12]:

- $\mathbf{R}\mathbf{R}^T = \mathbf{R}^T\mathbf{R} = \mathbf{I}_{3\times3}$, meaning that the determinant is ±1.
- Any matrix product of two elements in O(3) is also an element of it.
- Preserve the distance between both points (isometry).

The sub-group of proper orthogonal transformations are those with determinant $+1$, and is known as the Special Orthogonal Group SO(3). These are pure rotations in $\mathbb{R}^3$ that move a point or rotate the reference frame along a spherical manifold.

3.1.3 Euler Angles

Rotations can also be represented more intuitively using Euler angles. These are rotations about individual axes of the frame applied in a sequence, for example zyx (also known as yaw-pitch-roll). Applying an Euler angle rotation is equivalent to applying the SO(3) matrix product of all three single-axis rotations. However, note that the sequence of axes in the Euler angle rotations changes the final transformation as matrix operations are not commutative, and each singular axis rotation modifies the orientation of the reference frame.

The rotation matrices for rotation through angles α, β and γ which are anti-clockwise about the z, y and x axes, respectively, are as follows:

$$\mathbf{R_z} = \begin{bmatrix} \cos(\alpha) & -\sin(\alpha) & 0 \\ \sin(\alpha) & \cos(\alpha) & 0 \\ 0 & 0 & 1 \end{bmatrix} \tag{3.4}$$

$$\mathbf{R_y} = \begin{bmatrix} \cos(\beta) & 0 & \sin(\beta) \\ 0 & 1 & 0 \\ -\sin(\beta) & 0 & \cos(\beta) \end{bmatrix} \tag{3.5}$$

$$\mathbf{R_x} = \begin{bmatrix} 1 & 0 & 0 \\ 0 & \cos(\gamma) & -\sin(\gamma) \\ 0 & \sin(\gamma) & \cos(\gamma) \end{bmatrix} \tag{3.6}$$

Which leads to the combined matrix product rotation matrix for order zyx:

$$\mathbf{R} = \mathbf{R_z}\mathbf{R_y}\mathbf{R_x} \tag{3.7}$$

Successive applications of Euler angle rotations modify the frame for each transformation. Applying the previous zyx rotations in (3.7), for example, applies a rotation through an angle of α about the z-axis z_1, then rotates through an angle of β about the rotated y-axis y_2, and finally applies a rotation through an angle of γ about the twice-rotated x-axis x_3. While Euler Angles can be used to represent orientation, the mapping between any set of Euler Angle rotations α, β and γ and SO(3) rotation matrix is not unique. Furthermore, rotations of 180 degrees on any axis cause gimbal lock [12].

3.1.4 Axis-Angle Representation

According to Euler's rotation theorem, any rotation in $\mathbb{R}^3$can be represented by a rotation about a single axis through a fixed point (in this case the origin of the reference frame). The axis is known as an Euler axis and will be denoted as the normalised angular velocity vector $\tilde{\boldsymbol{\omega}}$ orthogonal to the plane of rotation. Its product with the rotation angle θ is known as the Axis-Angle representation of rotation, $\boldsymbol{\omega}$. The rotation matrix for an Axis-Angle rotation representation is efficiently computed through the Rodrigues' rotation formula (3.8).

$$R_{[\omega]_\times}(\theta) = e^{[\omega]_\times \theta} = \mathbf{I}_{3\times 3} + [\omega]_\times \sin\theta + {[\omega]_\times}^2(1 - \cos\theta) \tag{3.8}$$

Where $[\omega]_\times$ is the skew-symmetric matrix, formed from the angular components

defined in the angular axis vector $\tilde{\boldsymbol{\omega}}$ as follows (3.10):

$$\tilde{\boldsymbol{\omega}} = \begin{bmatrix} \omega_x \\ \omega_y \\ \omega_x \end{bmatrix} \tag{3.9}$$

$$[\omega]_\times = \begin{bmatrix} 0 & -\omega_z & \omega_y \\ \omega_z & 0 & -\omega_x \\ -\omega_y & \omega_x & 0 \end{bmatrix} \tag{3.10}$$

3.1.5 The Special Euclidean Group SE(3)

Representing a rigid body in the Euclidean space requires information on both position and orientation, known collectively as pose. The orientation can be thought of as the rotation that acts on the rigid body to rotate its reference frame from alignment with the world frame. A 4×4 transformation matrix $\mathbf{H}$ maps from the world frame to the rigid body frame, and is composed of the SO(3) rotation matrix $\mathbf{R}$ and the position vector $\mathbf{t}$:

$$\mathbf{H} = \begin{bmatrix} \mathbf{R} & \mathbf{t} \\ \mathbf{0}_{1\times 3} & 1 \end{bmatrix} \tag{3.11}$$

The fourth dimension represents the transformation in homogeneous coordinates, which is required for the matrix to both rotate and translate positions represented homogeneously in a reference frame. The homogeneous coordinate representation of a position in $\mathbb{R}^3$adds a fourth dimension '1' to the original $\mathbf{t}$ vector. The set of defined transformation matrices $\mathbf{H}$ containing proper rotations in SO(3) form the Special Euclidean Group SE(3).

3.1.6 Exponential and Logarithmic Maps of SO(3) and SE(3)

Corresponding to SO(3) and SE(3) are their Lie Algebras which are the tangent spaces at the identity element. The logarithm map is the mapping between the Lie Group and Lie Algebra, and is used as a more compact representation for a SO(3) and SE(3) matrix as it uses the same number of elements as degrees of freedom which reduces redundant matrix entries. The mapping from the Lie Algebra back to the Lie Group is known as the exponential map. Operations in Lie Algebra spaces involve more complex algebra than for the corresponding Lie Group Spaces (which can be calculated by purely using matrix operations). For this reason transformations on pose and positions are commonly applied on the Lie Group representations after converting from the Lie Algebra.

The Lie Algebra representation of SO(3) is denoted as $\mathfrak{so}(3)$, and is equivalent to the Axis-Angle representation of the rotation. The $\mathbb{R}^3$ position and $\mathfrak{so}(3)$ vectors together form the $\mathbb{R}^3 \times \mathfrak{so}(3)$ pose representation, which is composed of the translation vector $\mathbf{t}$ and Axis-Angle product representation $\boldsymbol{\omega}$:

$$\mathbf{x} = \begin{bmatrix} \mathbf{t} \\ \boldsymbol{\omega} \end{bmatrix} \tag{3.12}$$

The logarithm map ln : SO(3) $\mapsto \mathfrak{so}(3)$ can be efficiently computed using the inverse of the Rodrigues rotation formula in (3.8). If the rotation matrix R is the identity matrix there are infinite solutions of $\theta = 0$ angle rotations and any axis vector. If $tr(R) \geq -1$ there are two solutions for $\pi = 0$, which are $\tilde{\boldsymbol{\omega}}$ and $-\tilde{\boldsymbol{\omega}}$, and one of the two must be chosen arbitrarily. If $3 > tr(R) > -1$, the solution is unique for the range $-\pi < \theta < \pi$ (3.14).

$$\theta = \text{acos}\,\frac{tr(R) - 1}{2} \tag{3.13}$$

$$\tilde{\boldsymbol{\omega}} = \frac{1}{2\sin\theta} \begin{bmatrix} R(3,2) - R(2,3) \\ R(1,3) - R(1,3) \\ R(2,1) - R(1,2) \end{bmatrix} \tag{3.14}$$

The exponential map expanding the $\mathbb{R}^3 \times \mathfrak{so}(3)$ pose representation to an SE(3) matrix can be efficiently computed using the $\mathbf{t}$ vector component (first 3 entries of the $\mathbb{R}^3 \times \mathfrak{so}(3)$ pose) and expanding the Axis-Angle representation into the SO(3) matrix using the Rodrigues Rotation Formula (3.8).

The Lie Algebra for a SE(3) matrix (denoted here as Log(SE(3)) or $\mathfrak{se}(3)$) is defined as the following vector representation, where $\mathbf{t}'$ is the translation component and $\boldsymbol{\omega}$ is the rotation component:

$$\mathbf{v} = \begin{bmatrix} \mathbf{t}' \\ \boldsymbol{\omega} \end{bmatrix} \tag{3.15}$$

We define a 4×4 matrix $\mathbf{A}(\mathbf{v})$ as the following, where $[\omega]_\times$ is the skew symmetric matrix in (3.10):

$$\mathbf{A}(\mathbf{v}) = \begin{bmatrix} [\omega]_\times & \mathbf{t} \\ \mathbf{0}_{1\times 3} & 1 \end{bmatrix} \tag{3.16}$$

The exponential map $\mathfrak{se}(3) \mapsto$ SE(3) is fully defined for all of the domain of $\mathfrak{se}(3)$ and has a closed form. It is found using the exponential of $\mathbf{A}(\mathbf{v})$ [12].

$$e^{\mathbf{v}} \equiv e^{A(\mathbf{v})} = \begin{bmatrix} e^{[\omega]_\times} & \mathbf{Vt} \\ \mathbf{0_{1\times 3}} & 1 \end{bmatrix} \tag{3.17}$$

$$\mathbf{V} = \mathbf{I}_{3\times 3} + \frac{1 - \cos\theta}{\theta^2}[\omega]_\times + \frac{\theta - \sin\theta}{\theta^3}[\omega]_\times^2 \tag{3.18}$$

The logarithm mapping SE(3) $\mapsto \mathfrak{se}(3)$ in (3.15) is composed of the axis-angle representation of the 3×3 upper left SO(3) rotation matrix, found using the logarithm map SO(3) $\mapsto \mathfrak{so}(3)$ in (3.13). The translational component $\mathbf{v}$ is found by applying the inverse of $\mathbf{V}$ from (3.18):

$$\mathbf{t}' = \mathbf{V}^{-1}\mathbf{t} \tag{3.19}$$

3.2 Simultaneous Localisation and Mapping

3.2.1 Probabilistic Representation

The objective of solving the fundamental SLAM problem is to maximise the joint probability of the robot's trajectory and map given the robot initial state and sensor measurements obtained at each step. This can be represented a Bayesian belief net of conditional probabilities, where we estimate the current state of the robot (posterior) from the conditional probabilities of sensor measurements and robot control input given the initial state probability (prior). In global optimisation methods, all of the previous robot poses and sensor measurements constitute a joint probability [4].

The state constitutes the robot poses at each step, and the positions of points sensed and tracked in the environment. As is standard for SLAM algorithms, the variables in the state are modelled as being random. The robot poses at time step k is defined as a multivariate Gaussian random variable with mean values vector μ_{x_k} and covariances Σ_{x_k} (3.20).

$$x_k \sim \mathcal{N}(\mu_{x_k}, \Sigma_{x_k}) \tag{3.20}$$

Objects in the robot map are represented by points which are abstract representations of features on an object that can be sensed. Each point is variable z with index i in the map. These are also modelled as multivariate Gaussian random variables with mean vector μ_{z^i} and covariance Σ_{z^i}

$$z^i \sim \mathcal{N}(\mu_{z^i}, \Sigma_{z^i}) \tag{3.21}$$

Measurements are relationships between the state variables, modelled as conditional probabilities. In the standard SLAM algorithm, there are two types of measurements, which are the odometry and point measurements. The odometry is the transformation between two robot poses for time step k and $k-1$ from motion input o_k with independent zero-mean Gaussian noise v_k that has covariance Σ_{v_k}.

$$v_k \sim \mathcal{N}(0, \Sigma_{v_k}) \tag{3.22}$$

$$x_k = f(x_{k-1}, o_k) + v_k \tag{3.23}$$

The conditional probability of a robot's pose x_k given the previous pose x_{k-1}, using the odometry o_k as a measurement is as follows 3.24:

$$P(x_k|x_{k-1}, o_k) \propto \exp -\frac{1}{2}||f_i(x_k, x_{k-1}) - o_k||^2_{\Sigma_{v_k}} \tag{3.24}$$

Measurements of a point z^i_k are taken from a robot state x_k. The measurement model is a conditional probability of based on the current point estimation and the measurement value l^i_k, and the noise is also modelled as a zero-mean Gaussian random variable w^i_k with covariance Σ_{w_k}):

$$z^i_k = h_i(x_k, l^i_k) + w^i_k \tag{3.25}$$

$$P(z^i_k|x_k, l^i_k) \propto \exp -\frac{1}{2}||h_k(x_k, l^i_k) - z_k||^2_{\Sigma_{w_k}} \tag{3.26}$$

The joint probability model for all of the robot state transitions and point measurements is the product of all the conditional probabilities given a prior $P(x_0)$:

$$P(X, L, Z) = P(x_0) \prod_{k=1}^{mk} P(x_k|x_{k-1}, o_k) \prod_{i=1}^{mi} P(z^i|x_k, l^i_k) \tag{3.27}$$

3.2.2 Factor Graphs

A factor graph is a graphical representation of the probability distribution. It is composed of variables, and functions between the variables (called factors). Any variable can be expressed as a function its factors which are the functional relationships between it and other variables. Factor graphs are bipartite, meaning that all the variables can be divided into two independent sets with conditional dependencies between variables in both sets.

In the type of factor graph used in this SLAM problem, a vertex is a random variable that is part of the state. An edge is a factor that denotes a conditional probability between sets of vertices, such as a an odometry measurement (3.24) or point measurements (3.26). The edge type represents the function. The graph is constructed by first initialising all the vertexes from measurements, then finding the Maximum A Posteriori estimate for the joint probabilities model. An example factor graph for a map with three robot state and two points in the map is shown in Figure 3.2.

3.2.3 Non-Linear Least Squares (NLS) Optimisation

To find the Maximum A Posteriori estimate for the entire robot trajectory and environment point locations, we maximise the joint conditional probabilities of all

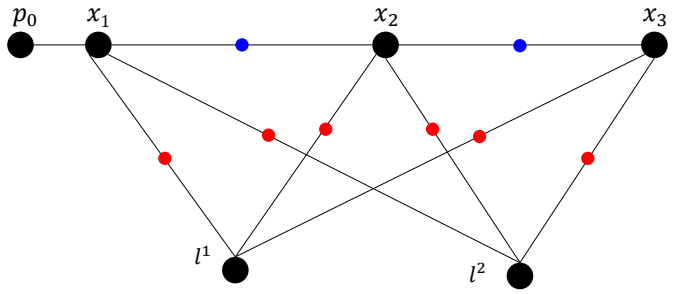

Figure 3.2: Factor Graph representation for the standard SLAM problem. Black circles indicate vertexes, and lines are edges. Red nodes are measurement factors, and blue odometry.

the robot poses X, and point locations L and robot-point sensor measurements L, which is $P(X, L, Z)$ (3.27). The log of $P(X, L, Z)$ is minimised instead as it is an easier computation, which yields the non-linear least squares problem in (3.28), where Θ^* is the vector of unknowns in (X,L).

$$\Theta^* = \underset{\Theta}{\operatorname{argmin}} \sum_{k=1}^{mk} ||f_k(x_k, x_{k-1}) - o_k||^2_{\Sigma_{v_k}} + \sum_{i=1}^{mi} ||h_i(x_k, l_k^i) - z_k||^2_{\Sigma_{w_k}} \tag{3.28}$$

The non-linear least squares problem is solved using iterative optimisation algorithms such as Gauss-Newton or Levenberg-Marquardt. The system represented by the factor graph is linearised for each iteration of the algorithm to form a linear least squares problem that is solved for in closed form by matrix factorization. Each iteration of the solution starts at a linearisation point at the current estimate Θ^0 and computes a small correction δ towards the solution. For a small enough $||\delta||$ Taylor series expansion is used to linearly approximate the neighbourhood of Θ^*.

The linearisation is done for each iteration of the non-linear least squares algorithm about a linearisation point by computing the Jacobians for each of the edges in the graph. (3.29) is the linearisation of (3.23), where (3.30) is the Jacobian, δx_{k-1} and δx_k are the linearisation steps, and a_k is the odometry prediction error between the predicted motion input and the actual odometry reading $a_k \triangleq x_k - f(x_{k-1}, o_k)$.

$$f_k(x_{k-1}, o_k) - x_k \approx \{f_k(x^0_{k-1}, o_k) + F^k_{k-1}\delta x_{k-1}\} - \{x^0_k + \delta x_k\} = \{F^{k-1}_k \delta x_{k-1} - \delta x_k\} - a_k \tag{3.29}$$

$$F^k_{k-1} \triangleq \left[\frac{\partial f_k(x_{k-1}, u_k)}{\partial x_{k-1}}\right]_{x^0_{k-1}} \tag{3.30}$$

The measurement model is linearised similar to (3.25), where z^i_k is the measured

value, and c_k^i is the measurement prediction error (3.31).

$$h_i(x_k, l_k^i) - z_k^i \approx h_i(x_k^0, l_{k_i}^0) + H_k^i \delta x_k + J_k^i \delta l_k^i - z_k^i = H_k^i \delta x_k + J_k^i \delta l_k^i - c_k^i \tag{3.31}$$

$$H_k^i \triangleq \left[\frac{\partial h_i(x_k, l_k^i)}{\partial x_k}\right]_{x_k^0, l_{k_i}^0} J_k^i \triangleq \left[\frac{\partial h_i^{-1}(x_k, l_k^i)}{\partial l_k^i}\right]_{x_k^0, l_{k_i}^0} \tag{3.32}$$

Replacing the original non-linear least squares functions with the linearised functions in (3.28) yields the linear least-squares optimisation:

$$\delta^* = \text{argmin}_\delta \left\{ \sum_{i=1}^{M} ||F_{k-1}^k \delta x_k + F_k^{k-1} \delta x_{k-1} - a_k||_{\Sigma_k}^2 + \sum_{k=1}^{K} ||H_k^i \delta x_k + J_k^i \delta l_k^i - c_k^i||_{\Sigma_{w_k}}^2 \right\} \tag{3.33}$$

The Square Root Smoothing optimisation method developed by Dellaert et. al [4] integrates Σ_k from (3.33) into the Jacobian matrix by pre-multiplying the Jacobian Matrices and residuals vector in the sums with the matrix square root transpose of its covariances $\Sigma_k^{-\top/2}$ and $\Sigma_{w_k}^{-\top/2}$. We then collect the Jacobians in a matrix A and the prediction errors at the current linearisation point into a residual vector $\mathbf{b}$, to obtain the standard least squares optimisation problem:

$$\delta^* = \underset{\delta}{\text{argmin}} \, ||A\delta - \mathbf{b}||_2^2 \tag{3.34}$$

As A has dimensionality $m \geq n$, the unique least squares solution can be found by solving the normal equations to compute the correction δ:

$$\delta^* = \underset{\delta}{\text{argmin}} \, ||A^\top A\delta - A^\top A\mathbf{b}||_\Sigma^2 \tag{3.35}$$

A is a matrix representation of the factor graph of the SLAM system. Each block in the matrix corresponds to a single edge between the relevant entries in its column and row indexes. Each set of rows in the residuals vector is the error adjustment for a vertex. At the end of each iteration, the vertex and edge values for the factor graph are recomputed, and a new linearisation point is determined by $\Theta^{k+1} = \Theta^k + \delta$. The system is iterated until the norm of the increment $||\delta^*||$ falls below a threshold.

The computing time for the solution depends on the sparsity and ordering of the matrix. A good variable ordering that maintains the sparsity of the matrix greatly improves the efficiency of the solver operation. This is usually done during the construction of the linear system Jacobian matrix A.

Chapter 4

Method

4.1 Concepts in DO-SLAM

The DO-SLAM Framework has two distinct parts that are separated conceptually, which are the front-end and the back-end.

The **front end** is the data generation or collection part of the DO-SLAM framework, which creates sensor measurements of the environment in a text format containing the measurements for the factor graph of the SLAM problem.

The **back end** is the solution part of the DO-SLAM framework, which constructs a graph representation of the SLAM problem consisting of vertices and edges from the graph file (explained in subsection 3.2.2), and uses non linear least squares optimisation to solve for the final estimate (see subsection 3.2.3).

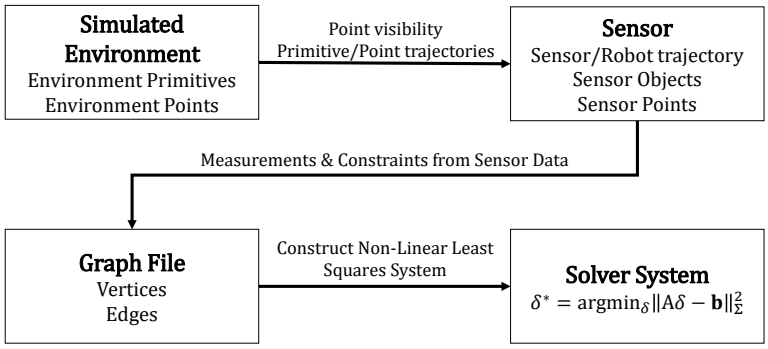

Figure 4.1: The DO-SLAM structure for the data generated by the simulated environment. The front end is the simulated environment and sensor. The back end is the graph file and solver.

Some key concepts required to understand the remainder of this chapter are explained in subsection 4.1.1.

4.1.1 Explanation of Key Terms in DO-SLAM

Front-end Generates data through a simulated environment or collects it from a real dataset, and processes it through an abstract sensor implementation

to create graph files: one with the noise-added measurements for the SLAM solution, and second with the fully constructed ground truth solution without noise (if possible).

Simulated Environment An abstract representation of the real world implemented purely through software, that can create simulated data to be read as sensor data for testing purposes. Consists of environment primitives and points that can model environment structure and have their own motion for the simulation time.

Primitive Abstract 2D or 3D shapes that model the real world, such as rectangles, planes or ellipsoids. They have a structure which is represented either through geometric properties (such as width, height or radius) or a mesh, and motion which is provided by a trajectory.

Mesh Models the surface of a primitive as 3D triangles that are used by the simulated environment sensor to implement occlusion between primitives in the simulated environment.

Robot Travels through the environment, and uses sensors to measure its own movement (known as odometry) and observe properties of objects and points in the environment (such as position, structure or motion).

Sensor Abstract representation of sensor device on a robot that is specialised to read information from a specific type of data source, for example the simulated environment or a depth camera, and create measurements for the graph file. The sensor has its own internal representation of the environment consisting of sensor objects and sensor points. For the simulated environment these are created by simulating a moving robot with sensor travelling through the simulated environment and creating sensor points and sensor objects from the environment primitive and environment point information. These are used along with the robot trajectory and sensor properties to construct measurements for the graph file.

Point Abstraction of a feature in the environment that can be sensed and tracked by a sensor. Points are initialised within the simulated environment or are extracted from real world data by the specialised sensor. If a point is static, it is represented as a single vertex in the factor graph with measurements from each robot pose where the point is visible in the robot sensor. If a point is dynamic, it is represented as a vertex for each step where it is observed with additional motion measurements or estimation between vertexes in successive steps.

Object Exists in the simulated or real environment and has features on its surface that are abstracted as points. Points on an object can be observed and tracked by a sensor to construct measurements, and additional information on the properties of an object or its relationship to associated points can be observed by a sensor and implemented as a constraint in the factor graph.

Graph File The text form of a factor graph for the SLAM system constructed from sensor measurements, consisting of an initial estimate for vertices which are variables in the environment, and measurement edges that are factors that have sensor noise.

Measurement The conditional probability of a sensor reading between two or more variables in the robot state, implemented as an edge in the factor graph. It has a value and covariance corresponding to the sensor noise. Measurements constructed by the sensor for the simulated environments have simulated noise.

Ground Truth The true data of the environment as a factor graph (vertices and edges), with no noise. This is created to evaluate the accuracy of the algorithm for the noisy sensor measurements and compare different point and motion models.

Constraint Additional information of the relationships between variables in the robot state, implemented as factors between their respective vertexes in the factor graph. DO-SLAM can implement structure constraints, such as associating static points to a plane [5], or in the context of this project associates points in different time steps to an estimated average velocity or constant motion (further explained in section 4.3).

Solver The non-linear least squares optimisation solution algorithm for the SLAM-system constructed from the factor graph.

The simulated environment, sensor, graph file and solver are separate abstract entities of their own, i.e. in a code implementation they are self-contained and encapsulate all the necessary information without requiring any external methods (the details on the implementation are in chapter chapter 5).

4.2 Modelling of Dynamic Rigid Bodies

A rigid body is defined as an object where the deformation of the internal structure of the body is non-existent or negligible, i.e. all points existing on the rigid body are fixed with respect to the object-fixed reference frame. We model a rigid body

as a reference frame in $\mathbb{R}^3$existing within the map and relative to the inertial frame. Let $\{0\}$ denote the inertial frame, and ${}^0X_k$ and ${}^0L_k^j$ the robot pose and an object pose with respect to the inertial frame respectively, where k is the time step, and j is the index of the object. ${}^0X_k$ and ${}^0L_k^j$ in SE(3) is also the transform mappings between the inertial frame and the robot/object frames.

Modelling the motion of a rigid body is done by applying the relative SE(3) transform of the object between time steps k and $k-1$ in the object fixed reference frame for time step k, denoted as ${}_{k-1}^{k}H_k^j$. The object pose in the inertial frame for time step k is obtained from the previous pose for time step $k-1$ and the motion input (4.1). This is also applicable for the robot where the motion is an odometry measurement represented in SE(3), which is the relative pose transform in the robot frame ${}_{k-1}^{k}H_k^x$ (4.2).

$$ {}^0L_k^j = {}^0L_{k-1}^j \; {}_{k-1}^{k}H_k^j \tag{4.1} $$

$$ {}^0X_k = {}^0X_{k-1} \; {}_{k-1}^{k}H_k^x \tag{4.2} $$

The transformation between any two poses in the inertial frame with respect to the first pose is given by the 'Absolute to Relative Pose' Transform. This is illustrated for an object observed in the robot frame ${}^0X$ (4.3). The motion input for an object between two time steps $k-1$ and k is another applied case (4.4). The odometry measurement for the robot is the same operation, for the robot poses ${}^0X_k$ and ${}^0X_{k-1}$.

$$ {}^X L_k^j = {}^0X_k{}^{-1} \, {}^0L_k^j \tag{4.3} $$

$$ {}_{k}^{k}H_{k+1}^j = {}^0L_{k-1}^j{}^{-1} \, {}^0L_k^j \tag{4.4} $$

The $\mathbb{R}^3$ position of a point existing on an object in its object reference frame is notated as ${}^L l_k^i$, where L is the frame of whatever object the point is part of (omitting the object index j), and i is the point index (which is unique for all the points in an environment). This is a homogeneous $\mathbb{R}^3$ position, to allow for matrix multiplication with the homogeneous SE(3) pose representation (see subsection 3.1.5). Its position in the inertial frame is obtained by applying the transform mapping between it and the object frame, which we will call 'Relative to Absolute Position' (4.5).

$$ {}^0l_k^i = {}^0L_k^j \, {}^L l_k^i \tag{4.5} $$

Similarly the point position in another non-inertial frame can be found from its equivalent inertial frame representation by applying the inverse of the object pose, called 'Absolute To Relative Position', shown in (4.6) for the object frame.

$$ {}^{L}l_k^i = {}^{0}L_k^{j\,-1}\,{}^{0}l_k^i \tag{4.6} $$

These geometric relationships are summarised visually in Figure 4.2, for a single object with frame L.

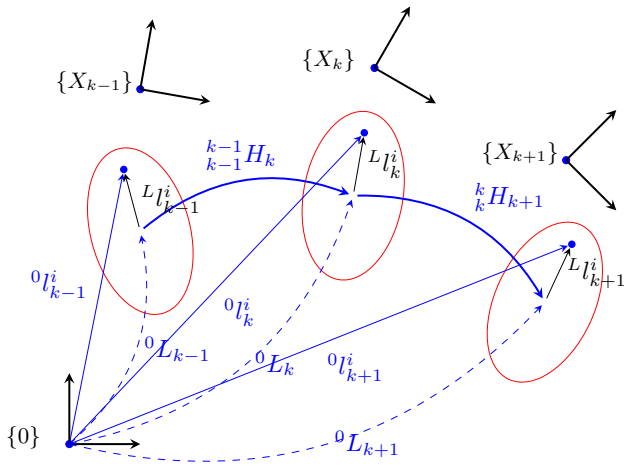

Figure 4.2: Representative coordinates of the rigid body in motion. The points ${}^{L}l^i$ are represented relative to the rigid body centre of mass L at each step. Source: [2]

4.3 Measurements and Constraints

We now link the transformations described in section 4.2 to the Factor Graph representation described in subsection 3.2.2 in order to implement the non-linear least squares algorithm shown in subsection 3.2.3. Points and robot poses are vertices of the factor graph, with values in $\mathbb{R}^3$ and $\mathbb{R}^3\times$SO(3) (which is converted to SE(3) for operations) respectively. Measurements are edges between vertices, where the type encodes particular factor or function between the vertices and value is the measured value which includes the noise from the sensor creating the measurement.

Vertices and edges have covariances as they are multivariate Gaussian probabilities. Each edge type has a corresponding Jacobian function for the factor functions it implements, which is needed to linearise the measurement models when constructing the linear system.

The basic implementation of the DO-SLAM framework has two types of vertices: robot pose and point. A robot pose has a $\mathbb{R}^3\times$SO(3) representation which is converted into its SE(3) matrix equivalent using (3.8) and (3.11) for calculations. It has a 6×6 covariance matrix for the combinations of its 6 $\mathbb{R}^3\times$SO(3) value entries. A point is in $\mathbb{R}^3$, with a 3×3 covariance matrix. The edge covariances have the dimensionality of the factor function.

A basic SLAM algorithm only has 2 types of measurements, 1) an odometry measurement which is a relative pose (4.3) for ${}_{k-1}^{k}X_k$), and 2) a static point being sensed by the robot. The latter is the position $\mathbb{R}^3$ position in the robot-frame, and is obtained by applying (4.6) for the specific case of a point observed in the robot frame (4.7). The Jacobian matrix for a relative pose measurement (4.3) is numerically approximated by applying a small perturbation motion input ϵ and computing the pose differences divided by the perturbation input.

$$ {}^{k}y_k^i = {}^{0}X_k^{-1}\,{}^{0}l_k^i \tag{4.7} $$

Every measurement in the factor graph has Gaussian noise added it according to the covariance matrix of the edge type. This is added after the measurement is created from the applying the function on the actual point or pose values, as the noise for a measurement is independent from previous measurements taken. Dynamic motion of points are implemented as additional vertices with edges between the vertices belonging to the moving point in consecutive time steps, and the values are the residuals of the cost minimization for the motion measurement function. The error of a static points' estimation is reduced over time through multiple sensor measurements of it in different time steps, which creates additional edges between robot poses and itself. For a point on a dynamic rigid body object, separate vertices are required for each time step, and more information is added in the form of motion measurements, which are explained in section 4.5.

4.4 Visibility Modelling

For the front-end simulated environment in the DO-SLAM framework, the measurements of points from a robot sensor in the simulated environment depend on whether they are visible in the sensor model. The base simulated sensor model is that of a visual and depth camera that provides direct $\mathbb{R}^3$ position of a point in the environment in the robot-frame. The position of the point is then converted to spherical coordinates (3.2) Points are deemed 'visible' if they are within the set field of view for the camera (given as spherical coordinate ranges in azimuth, elevation and radius).

The second stage of development for this sensor models occlusion done by rigid body objects in the simulated environment. This includes an abstract appearance model for a rigid body, and a technique to implement intra and inter object occlusion.

In an environment primitive, the structure of its surface is represented as a mesh of 3D-triangles, where each triangle is composed of 3 corners which are positions in $\mathbb{R}^3$ (similar to points) expressed in the object frame. For a mesh, each triangle

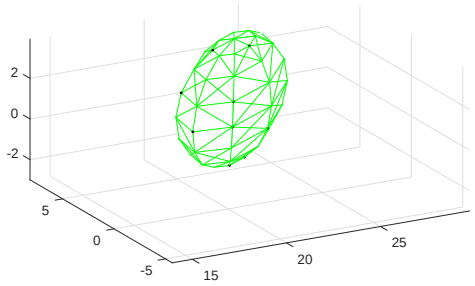

Figure 4.3: An environment primitive. The green wireframe shows the mesh, and black dots are points on the primitive that exist in the environment and are sensed.

is a set of the 3 corners, set when the structure of the primitive is initialised (the details on the implementation are explained in subsection 5.1.4). Points exist on this surface either at the same position as corners or along the planar surface of the triangles. This is illustrated graphically in Figure 4.3.

To set visibility, all of the points within the sensor field of view are ray-intersected with the all of the triangles for rigid bodies also within the sensor field of view. If the ray of the point to the camera intersects any of the triangles and the intersection position is behind the triangle, the point is deemed not visible.

First, the position of corners for the triangles in a mesh are converted from the object-frame to the robot-frame, where p^n is a corner for $n = 1 : 3$ belonging to any triangle in an object j's mesh. Note that a point in the mesh structure p^n does not necessarily exist in the environment as a sensed point l^j, however it does exist within the rigid body object appearance model for the purpose of occlusion. (4.8) is the mesh corner position in the inertial frame given the pose of its parent object j at time step k, L_k^j. Note that this results in the corner having a time index k as its inertial frame position is not constant due to the movement of its object. (4.9) is the corner position in the robot-frame.

$$ {}^0p_k^n = {}^0L_k^j \, {}^L p^n \tag{4.8} $$

$$ {}^k p_k^n = {}^0X_k{}^{-1} \, {}^0p_k^n \tag{4.9} $$

These equations extract the robot-frame positions of all 3 corners in a mesh triangle, which will be notated as p_1, p_2 and p_3 from here on. A point in the environment with index i sensed by the robot sensor in the robot-frame, ${}^k l_k^i$, an has a ray to the sensor position q - this is the same as the $\mathbb{R}^3$ position vector itself as the origin of the robot in its own frame is $[0, 0, 0]^\top$.

For the 3 triangle corners p^1, p^2 and p^3, and ray from the point to the camera q, first check the intersection position p^0 between the infinite plane of the triangle and the point ray by finding the normal to the triangle, N:

$$N = (p^2 - p^1) \times (p^3 - p^1) \tag{4.10}$$

$$p^0 = (p^1 \cdot N)/((q \cdot N) \times q) \tag{4.11}$$

Then we check whether the point exists within the perimeter of the triangle, which fulfils the following conditions:

$$((p^2 - p^1) \times (p^0 - p^1)) \cdot N > 0 \tag{4.12}$$

$$((p^3 - p^2) \times (p^0 - p^2)) \cdot N > 0 \tag{4.13}$$

$$((p^1 - p^3) \times (p^0 - p^3)) \cdot N > 0 \tag{4.14}$$

However this method of intersection also results in the conditions in (4.12) (4.13) and (4.14) being 'true' for points in front of the triangle where the ray vector intersects behind it. To check whether the point of intersection is in front of the point ray or behind, we check whether the intersection position of the ray and the mesh triangle is behind or in front of the triangle by comparing their euclidean distances from the sensor frame origin. All of the steps mentioned earlier are summarised in the following pseudo-code for a single time step k:

1. Iterate through all the mesh corners of the objects p^n where n is the index of a corner in an object. For every corner:
    1.1. Find the positions of the corners in the robot frame ${}^k p^n$.
2. Compile all the sets of mesh corners belonging to the mesh-triangles in an array m.
3. For every point in the environment observed in the robot-frame ${}^k p_k^i$:
    3.1. Set visibility to ON.
    3.2. Iterate though all the rows in array m (each being a mesh triangle), comprising of 3 mesh corner positions p^1, p^2 and p^3.
        3.2.1. Find the normal to the triangle, N (4.10).
        3.2.2. Intersect the ray between the sensor origin and point position q with infinite plane of the triangle N (4.11) to find the intersection p^0.
        3.2.3. IF the point exists within the perimeter of the triangle, checked by the conditions in (4.12) (4.13) (4.14):
            3.2.3.1. Check the euclidean distances $|p^0| < |q|$, set visibility to 'OFF' if TRUE.
        3.2.4. ELSE continue to next row in array m.

4.5 Point Motion Measurements and Constraints

The standard non-linear least squares based SLAM algorithm implements measurement edges from multiple robot poses to a single point vertex as it assumes that the points are static. However, this case breaks down in a dynamic environment as points are also moving with respect to the inertial frame due to the movement of objects they are part of. Therefore, each point estimation in the robot map is a separate point vertex for the point's $\mathbb{R}^3$ position at time step k. If the environment consists of purely dynamic points, without any additional information in the Factor Graph, no optimisation can be conducted on this system as the information matrix A only has edges between consecutive poses and singular measurements of each point for each time step from a pose.

The DO-SLAM framework tests methods of incorporating independent measurement and estimation of the *motion* of points into the SLAM solver. These are implemented as either motion measurements, which are edges between point vertexes, or motion estimations which are vertices. Five motion measurement types and one estimation are tested in this honours thesis.

4.5.1 2-point Edge

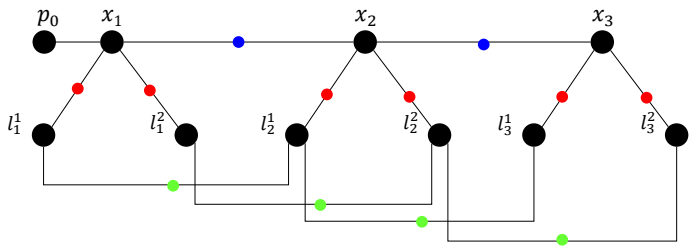

Figure 4.4: Factor Graph for the 2-point edge. Black cirles are vertices and lines are edges. The red nodes are odometry measurement factors, blue nodes are point measurement factors, and green nodes are 2-point motion measurement factors.

We begin with the most specific measurement of the absolute motion of a single point's motion between any two time steps, which we will call the 2-point edge.

The 2-point edge is a motion measurement of the absolute position difference, which is a vector in $\mathbb{R}^3$, between any two point vertices. In the context of the robot map, this is the inertial frame motion difference $\mathbf{d}$ estimated between the positions of a moving point from one time step to the next ${}^0l_k$ and ${}^0l_{k-1}$. This point motion measurement edge is *independent* from the robot-point sensor observation, and has its own covariance, initialised as a diagonal of the variances for the motion in each $\mathbb{R}^3$ dimension x, y and z. The value of the edge is the $\mathbf{d}$ vector between the point

positions for time steps k and $k-1$ (4.15). The factor graph for this measurement is shown in Figure 4.4. The points are not associated to an object in this graph, and data association between the point vertices for the consecutive time steps is assumed.

$$\mathbf{d} = {}^{0}l_k - {}^{0}l_{k-1} \tag{4.15}$$

The two edge Jacobians for this edge are the positive and negative linear identity matrices:

$$\frac{\partial \mathbf{d}}{\partial {}^{\mathbf{0}}l_k} = \mathbf{I}_{3\times 3} \qquad \frac{\partial \mathbf{d}}{\partial {}^{\mathbf{0}}l_{k-1}} = -\mathbf{I}_{3\times 3} \tag{4.16}$$

The 2-point edge is the first motion measurement we implement, and represents the most unrealistic scenario where we do not assume any motion model for the point trajectory, an an exact inertial frame measurement of a point's translation between two time steps can be provided by a sensor. We omit the scalar version of this implementation (a point euclidean distance) due to the infeasibility of such a sensor.

4.5.2 3-point Edge

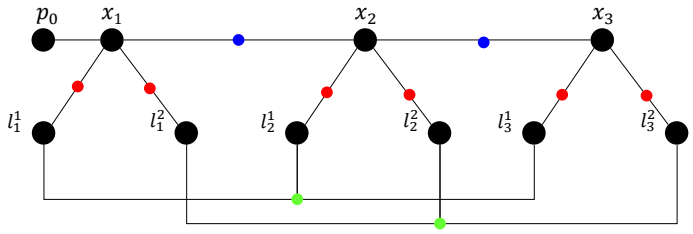

Figure 4.5: Factor Graph for the 3-point edge. Black cirles are vertices and lines are edges. The red nodes are odometry measurement factors, blue nodes are point measurement factors, and green nodes are 3-point motion measurement factors.

The 3-point edge expands on the 2-point edge by making an linear motion assumption for a point's trajectory over three consecutive time steps. The measurement minimises the difference in the motions between time steps $(k, k-1)$ and $(k-1, k-2)$, denoted here as $\mathbf{d}_2$ (4.17), i.e. assuming that the point has *constant linear motion*. We also test this in its scalar form (4.18) which is the distance measurement of the point's motion for three consecutive time steps, d_2. The scalar form is a more realistic case of the sort of measurement a real motion sensor can provide compared to the absolute inertial frame translation.

The values for the edges are created from the point positions, and have noise added independently of the sensor-point measurements. The factor graph is shown in Figure 4.5. This type of measurement is also unrealistic from a real world sensor point of view, but it allows us to test the validity of a rudimentary motion model assumption.

$$({}^0l_k - {}^0l_{k-1}) - ({}^0l_{k-1} - {}^0l_{k-2}) = \mathbf{d}_2 \tag{4.17}$$

$$||{}^0l_k - {}^0l_{k-1}|| - ||{}^0l_{k-1}{}^0l_{k-2}|| = d_2 \tag{4.18}$$

The Jacobians for (4.17) are shown in (4.19) and the Jacobians for (4.18) are shown in (4.20).

$$\frac{\partial \mathbf{d}_2}{\partial {}^0l_k} = \mathbf{I}_{3\times 3} \qquad \frac{\partial \mathbf{d}_2}{\partial {}^0l_{k-1}} = -2 \cdot \mathbf{I}_{3\times 3} \qquad \frac{\partial \mathbf{d}_2}{\partial {}^0l_{k-2}} = \mathbf{I}_{3\times 3} \tag{4.19}$$

$$\frac{\partial \mathbf{d}_2}{\partial {}^0l_k} = \left[-\text{sgn}({}^0l_k - {}^0l_{k-1})\right]^\top \quad \frac{\partial \mathbf{d}_2}{\partial {}^0l_{k-1}} = \begin{matrix}[\text{sgn}({}^0l_k - {}^0l_{k-1}) \\ -\text{sgn}({}^0l_{k-1} - {}^0l_{k-2})]^\top\end{matrix} \quad \frac{\partial \mathbf{d}_2}{\partial {}^0l_{k-2}} = \left[-\text{sgn}({}^0l_{k-1} - {}^0l_{k-2})\right]^\top \tag{4.20}$$

4.5.3 Velocity Vertex

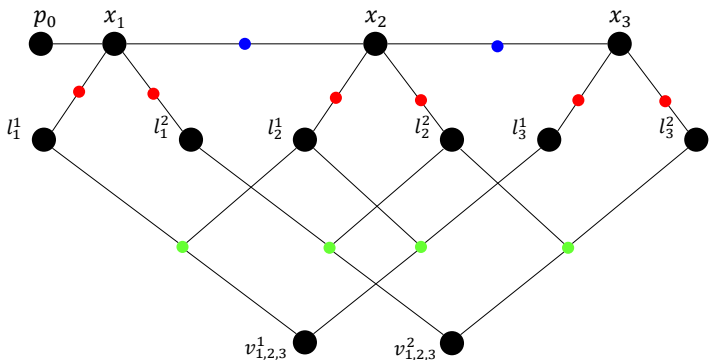

Figure 4.6: Factor Graph for the velocity vertex. Black cirles are vertices and lines are edges. The red dots are odometry measurement factors, blue edges are point measurement factors, and green are velocity-point position constraint factors.

The velocity vertex implements a *constant average linear integrated velocity* measurement between 2 pairs of 3 consecutive time steps $(k, k-1)$ and $(k-2, k-3)$. Each velocity vertex is an average integrated velocity vector or integrated speed (the norm of the velocity) over 3 consecutive time steps, which is independently initialised by taking the average integrated velocities of the point's motion. Each edge has

at least 3 vertices: the velocity vertex, and pairs of point vertices whose integrated velocity is being estimated. The edge value minimises the residual of the constraint $\mathbf{d}_3$.

The vector of the velocity is implemented as an $\mathbb{R}^3$ value (4.21), with the edges constraining the position of the points ${}^0l_k$, ${}^0l_{k-1}$, and ${}^0l_{k-2}$ by the estimated velocity. The factor graph is shown in Figure 4.6.

$$\mathbf{v} = \frac{({}^0l_k - {}^0l_{k-1}) + ({}^0l_{k-2} - {}^0l_{k-3})}{2} \tag{4.21}$$

$$\mathbf{v} - ({}^0l_k - {}^0l_{k-1}) = \mathbf{d}_3 \tag{4.22}$$

$$\mathbf{v} - ({}^0l_{k-1} - {}^0l_{k-2}) = \mathbf{d}_3 \tag{4.23}$$

The scalar of the integrated velocity, that is average distance, is implemented as the norm of the average integrated velocities.

$$v = \frac{||({}^0l_k - {}^0l_{k-1}|| + ||{}^0l_{k-2} - {}^0l_{k-3}||}{2} \tag{4.24}$$

$$v - ||{}^0l_k - {}^0l_{k-1}|| - v = 0 \tag{4.25}$$

$$v - ||{}^0l_{k-1} - {}^0l_{k-2}|| = 0 \tag{4.26}$$

The Jacobians for (4.22) and (4.23) are shown in (4.27). The scalar vertex implementation (4.24) for the edges (4.22) and (4.23) Jacobians are shown in (4.28).

$$\frac{\partial \mathbf{d}_3}{\partial \mathbf{v}} = \mathbf{I}_{3\times 3} \qquad \frac{\partial \mathbf{d}_3}{\partial {}^0l_k} = -\mathbf{I}_{3\times 3} \qquad \frac{\partial \mathbf{d}_3}{\partial {}^0l_{k-1}} = \mathbf{I}_{3\times 3} \tag{4.27}$$

$$\frac{\partial \mathbf{d}_3}{\partial v} = 1 \qquad \frac{\partial \mathbf{d}_3}{\partial {}^0l_k} = \left[-\text{sgn}({}^0l_k - {}^0l_{k-1})\right]^\top \qquad \frac{\partial \mathbf{d}_3}{\partial {}^0l_{k-1}} = \left[\text{sgn}({}^0l_{k-1} - {}^0l_{k-2})\right]^\top \tag{4.28}$$

4.5.4 Constant Motion

The point motion measurements and constraints described in subsection 4.5.1, subsection 4.5.2 and subsection 4.5.3 are all only applicable under a *constant linear motion*assumption. For points on a moving rigid-body, this assumption is only valid if the rigid body also has constant linear motion. We now expand the point motion estimation to a more general case, that where the object has a *constant motion* composed of a constant rotation and constant translation. The full derivation is in [2]. The factor graph representing a SLAM problem which integrates a constant SE(3) motion constraint is shown in Figure 4.8.

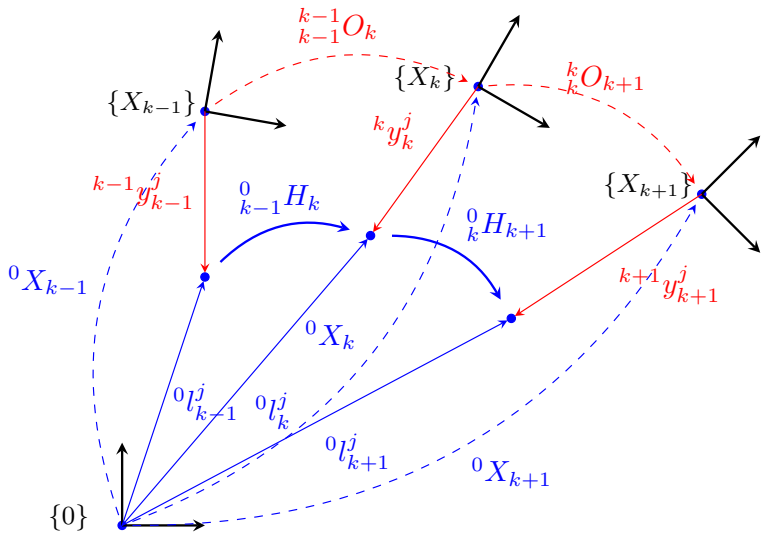

Figure 4.7: Representative coordinates of the SLAM system. Blue represents state elements and red the measurements. The relative poses have the corresponding notation: ${}^a_bH_c$, meaning that the relative pose of frame c with respect to frame b (the reference) is expressed in the coordinates of frame a. Source: [2].

Using (4.7), (4.5), and (4.4) we obtain the following relationship (for only one object with frame L):

$$ {}^0_kX_k\,{}^ky^i_k = {}^0L_{k+1}\ {}^k_kH_{k+1}{}^{-1}\ {}^Ll^i_k \tag{4.29}$$

The pose change for the object can be obtained in the inertial frame through the following relationship :

$$ {}^0_kH_{k+1} = {}^0L_k\ {}^k_kH_{k+1}{}^{-1}\ {}^0L_{k+1}{}^{-1} \tag{4.30}$$

This object pose change in the inertial frame is used to obtain the point location in the inertial frame:

$$ {}^0l^i_k = {}^0_kH^{-1}_{k+1}\ \ {}^0l^i_{k+1} \tag{4.31}$$

As we are assuming a constant motion model for the object it the object frame ${}^k_{k-1}H_k = {}^k_kH_{k+1} = C$, this also translates into constant motion of the object in the inertial frame:

$$ {}^0_kH_{k+1} = {}^0L_k\ \ C\ \ {}^0L_k{}^{-1} \tag{4.32}$$

The constant motion constraint function is (4.33), where ${}^0u^j = \log({}^0H^j)$, ${}^0H^j = [{}^0R^j\ {}^0t^j]$, and q_{s_j} is the Gaussian distributed process noise.

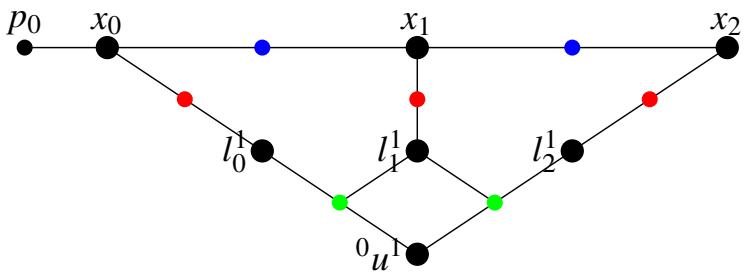

Figure 4.8: Factor Graph for the Constant Motion Vertex. Black cirles are vertices and lines are edges. The red nodes are odometry measurement factors, blue nodes are point measurement factors, and green nodes are motion-point position constraint factors. Source: [2].

$$g(l_k^i, l_{k+1}^i, {}^0u^j) = {}^0R^{j\top} {}^0l_{k+1}^i - {}^0R^{j\top} {}^0t^j - {}^0l_k^i + q_{s_j} \tag{4.33}$$

Chapter 5

Implementation

5.1 DO-SLAM Front End

DO-SLAM is implemented in MATLAB using Object Oriented Programming (OOP) Principles. Each part of the framework shown in Figure 4.1 and described in section 4.1 is implemented as its own abstract parent class. Child classes inherit from these parent classes to implement specific functionalities, and these are used in the high-end application of the frameworks. Additional supporting 'utils' are provided that abstract common shared properties and behaviours of entities existing within these classes.

The following sections discuss the properties and methods contained in the classes coded as part of DO-SLAM. All the classes exhibit encapsulation, where all of the required interaction with that class can be obtained through calling specialised methods, and the class is able to provide information in different formats as required by the invocation of those methods to make it robust for different uses.

A key property of all of the classes in the following sections is inheritance from the class '**ArrayGet&Set'**. This class sets common 'get' and 'set' methods that are robust to the type of property. The first argument provided when calling the 'get' method is the property called, and the remaining arguments are the specific input arguments required for that property. For properties that are arrays in MATLAB, 'ArrayGet&Set' is able to take the indexes of array entries required as input and output them as an object array. 'ArrayGet&Set' calls a 'getSwitch' method that exists in each inheriting class when it does not have the functionality to provide the desired property called, and allows for the inheriting class to provide its own additional 'get' functionality on top of the generic functionality provided by it. The main benefit of this class is that a particular type of get method can be applied to multiple class instances that are part of an object array and all of their respective values for the property queried can be obtained simultaneously.

5.1.1 Config

The 'config' class contains the standard information required by both the front-end and back-end to generate a simulated environment, create sensor measurements of it, output ground truth and sensor measurements graph files, read these graph files and solve the system. It has no direct methods of its own, however its properties are used as input by other classes. Key properties of 'config' include:

Filepaths and names 'measurementFileName' and 'groundTruthFileName' which are graph files that the sensors output to, and the back-end reads.

Pose Parametrisation named 'poseParameterisation'. The representation used for poses in euclidean space, which is currently either $\mathbb{R}^3 \times \mathfrak{so}(3)$ (set as string value 'R3xso3') or $\mathfrak{se}(3)$ (set as string value 'LogSE3').

Transform Function Handles These provide the function inputs for the transforms defined in section 4.2 based on 'poseParameterisation', which are 'absoluteToRelativePoseHandle' (4.3), 'absoluteToRelativePointHandle' (4.6), 'relativeToAbsolutePoseHandle' (4.2) and 'relativeToAbsolutePointHandle' (4.5).

Labels These are the labels of the different vertexes and edges in the graph file created by the abstract sensor and read by the graph class, named in the format '__Label'. For example, the label for a point vertex is 'pointVertexLabel' and edge between a robot pose and a point (which is a robot camera sensor measurement) is 'posePointEdgeLabel'.

Standard Deviations and Covariances The standard deviations of the Gaussian noise for edges, named 'std__'. They are column arrays with the dimensionality of the value of the edge. For example, the robot odometry edge standard deviation is a 6×1 vector 'stdPosePose'. Covariance matrices are automatically constructed from these standard deviations (with the assumption of independence between different dimensions), and stored as dependent properties 'cov__'.

Point Motion Model named 'pointMotionMeasurement', sets the type of point motion measurement or estimation for the sensor and solver, as explained in section 4.5. 'motionModel' determines whether the edges and vertices implemented are scalar ('speed') or vectors ('velocity').

Solver Settings which are 'solverType', 'solveRate', 'threshold' which is the norm of the residual vector that determines convergence of the solution, 'maxIterations' for the solver before it stops the NLS optimisation algorithm,

'maxNormDX' which is the maximum value of the residuals vector norm $||\delta X||$ (indicating divergence form the solution).

Camera Settings these are the camera field of view and range in spherical coordinates.

Dimensionality of points 'dimPoint' and poses 'dimPoint', used to initialise the empty Jacobian matrix A before vertices and edges are populated.

5.1.2 Geometric Representations

These implement representations described in section 3.1. The class abstracting any generic pose is "GP_Pose" and a point is "GP_Point". These two classes hold the base functionality for the implementation of environment points, environment primitives, sensor points and sensor objects.

GP_Pose can take an input pose in $\mathbb{R}^3 \times \mathfrak{so}(3)$, $\mathfrak{se}(3)$, or SE(3) representation, and output in those representations or give the axis-angle vector or rotation matrix as specified by the arguments provided in the 'get' or 'set' call. We define 'absolute pose' as the pose of a robot or object in the environment with respect to the inertial frame, and 'relative pose' as the relative transform between any two poses in the inertial frame, with respect to the first frame. The method 'AbsoluteToRelativePose' gives the relative pose between the GP_Pose and another GP_Pose given as input. The method 'RelativeToAbsolutePose' gives the absolute pose of the input GP_Pose argument with the invoking GP_Pose instance acting as a relative pose.

GP_Point is the position of any generic point in $\mathbb{R}^3$ with respect to the inertial, robot or object frames. It has a method to output its position with respect to the inertial frame if it is specified in a different frame through the 'RelativeToAbsolutePosition' method (4.1). It can also output its position in another frame if its position has been specified in the inertial frame by the 'AbsoluteToRelativePosition' method (4.6).

Both GP_Pose and GP_Point can add noise to their value properties according to the noise settings in the config. The current implementation only includes Gaussian noise.

5.1.3 Trajectories

Trajectories are used to model the motion of an object, point or the robot. They encapsulate all of the motion information required to model a primitive, point or object and create sensor measurements from it. The abstract parent class is simply called

"Trajectory" and its properties are inherited by its child classes "PoseTrajectory" and "PointTrajectory".

"PoseTrajectory" models a moving object with its own frame in the world, as described in section 4.2. It can be queried to obtain the pose of the object at an input time through the 'get' method, and give that pose with respect to any other input frame as a relative or absolute pose. It can also output the inertial frame relative transform between poses in two time steps (4.32). Pose Trajectory has a 'plot' method which shows the trajectory for the input time steps as a dotted line and axes. "PoseTrajectory" is not directly instantiated and acts as the abstract parent class containing necessary functionality for implementations of specific types of trajectories.

"PositionModelPointTrajectory" is a child class of "PoseTrajectory" that interpolates a continuous trajectory for a given input $\mathbb{R}^3$ waypoints over specified time steps. It fits a curve to the input time (t) and $\mathbb{R}^3$ coordinate positions using the MATLAB curve fitting toolbox, and calculates the orientation according to an assumed model where the trajectory frame x-axis points in the direction of motion and the z-axis is aligned to be as slose to normal to the yz-plane as possible. When a pose for an input time is queried by the 'get' method, the pose is interpolated according to the curve fitting the waypoints, therefore the pose can be queried for any time value.

"DiscretePoseTrajectory" is a child class of "PoseTrajectory" which stores GP_Poses for discrete time steps. Its main application is to implement a constant motion model for objects, which is done by its child class "ConstantMotionTrajectory" that takes in input a vector of time steps, an initial pose, and a constant motion transform (represented in $\mathbb{R}^3 \times \mathfrak{so}(3)$, $\mathfrak{se}(3)$, or $SE(3)$). It applies the constant motion transform successively for each time step, and stores it in an array. Constant SE(3) motion models are difficult to interpolate or integrate continuously, so storing the trajectory as discrete poses simplified this process.

"PointTrajectory" is similar to "PoseTrajectory" but only implements motion as $\mathbb{R}^3$ position without orientation. It is used to model the motion of points existing in the environment which may or may not pertain to objects. "PositionModelPointTrajectory" is the same as "PositionModelPoseTrajectory" but does not estimate any orientation. "DiscretePointTrajectory" is similar to the pure position data of "DiscretePoseTrajectory".

Trajectories can also be relative to another pose trajectory, which can model points associated to objects in the environment. "RelativePointTrajectory" is a child of "PointTrajectory" that takes a GP_Point relative position in the parent object frame, and the pose trajectory of that object as input. Its output poses are given as inertial frame positions of the point for the time step queried by applying

(4.5). Similarly "RelativePoseTrajectory" takes a parent object trajectory and a object frame pose as input, and outputs the inertial frame poses of the point for the queried time step by applying (4.1).

Static objects and points have "StaticPoseTrajectory" and "StaticPointTrajectory" as their trajectory property, which gives the same pose or position for any queried time step. They are interacted with using the same 'get' method calls as dynamic trajectories.

5.1.4 Simulated Environment

The simulated environment consists of environment points and environment primitives (which are defined in section 4.1). Each environment point has a unique index in the environment, and can be associated to a primitive with its own unique index. These indexes are set when primitives and points are instantiated as part of the environment.

The "EnvironmentPoint" class has properties 'index' (of itself in the environment, which is unique for all points), 'trajectory' which holds the point trajectory and 'primitiveIndexes' for its associated primitives (if any).

The parent "EnvironmentPrimitive" class has properties 'index' (of itself in the environment, unique for all primitives), 'trajectory' and 'pointIndexes' which are the environment indexes of points belonging to it in the environment. Primitives and points are added with automatic indexing in the environment when methods creating primitives are called in the environment class.

Of interest in this project are the rigid body environment primitives, which are called 'EP_Default'. They also have te additional properties 'MeshPoints' which are the corners for the triangles representing the mesh, and 'MeshLinks' which are the indexes for sets of point belonging the 3D triangles representing the surface of the primitive. EP_Default has methods that find the mesh corners in their object frame or the inertial frame for a given time step, and compile them as an array of GP_Points for output. Similarly it can do the additional step of outputting an array of mesh triangles, where each row contains the corner positions in a triangle (see section 4.4).

Specific types of primitives are instances of 'EP_Default' instantiated using specialised methods in the environment. The two implemented in this project are Ellipsoid and Cube. The methods "addEllipsoid" instantiates an ellipsoid according to the input parameters as its EP_Default and Environment Point class instances in the environment. The input is $[x, y, z]$ radii, resolution n, and trajectory, to create an EP_Default using the following steps:

1. Generate the ellipsoid surface corners with the radii and resolution input ar-

guments by using the Matlab ellipsoid function. This is a meshgrid output.

2. Find all of the corners for the mesh and the 'meshLinks' for the triangles through Delaunay triangulation (the Matlab function 'delaunay') on the positions generated by the meshgrid.

3. Create an array of GP_Points from all of the mesh corner positions, and sample 20% of them to abstract features on the surface that are part of the environment as EnvironmentPoint class instances.

4. Set the corner position GP_Point class array as the 'meshPoints' property and sets of index corners for mesh triangles as 'meshLinks' property in the primitive.

5. Create the 'RelativePointTrajectory' based on the input trajectory for all of the environment points.

6. Set environment indexes for the primitive and its points and add to the environment class properties 'environmentPoints' and 'environmentPrimitives' (done via a private method called on self 'addPrimitiveAndPoints').

EP_Default also has an internal plot method that displays its mesh as a 3D wireframe for the input time step. This is used for viewing the simulated environment (Figure 4.3).

The environment also has plot methods for itself, which calls the EP_Default plot method and plots the environment points. It can animate the figure by sequentially plotting the environment for an input array of time steps.

5.1.5 Sensors

The abstract parent class for all of the specialised sensor implementations is called "Sensor" and has a property 'trajectory', and is typically set as the trajectory of the sensor travelling through the simulated environment, which is a "RelativeTrajectory"' class instance initialised from the relative pose of the sensor with respect to the robot frame and the robot trajectory. The base sensor to read simulated environment data is called "SimulatedEnvironmentSensor" and inherits from "Sensor". "Sensor" and its child classes contain "SensorObjects" and "Points" which are the sensor's internal abstract representations of objects and points in the real environment, or environment primitives and environment points in the simulated environment.

For the purposes of generating simulated data, the structure and properties of environment points and primitives are similar to that of sensor points and objects, in that they have the same unique indexing and properties to reference associations

between each other. The 'addEnvironment' method takes an environment instance as input and creates sensor objects and points from the environment points and primitives, creating an internal sensor representation of the environment. Different primitive types are read into their appropriate sensor object class type by checking the primitive class types and calling the specialised method for it. The "SensorObject" class has subclasses "GeometryObject" and "RigidBodyObject". EP_Defaults are used to construct "RigidBodyObject" class instances when the simulated environment is read into the sensor. The sensor object subclasses are abstract representations of objects in the environment, and sensors operating on different data sources will have their own specialised functions to create these sensor objects from the data.

"Points" in the sensor have properties 'index', 'trajectory', 'objectIndexes' and 'vertexIndexes', which are the same as environment points (described in subsection 5.1.4). The 'vertexIndexes' property stores the indexes of the vertices in the graph file during measurements generation. Indexing from the environment points to sensor points and from environment primitives to sensor objects is identical for the convenience of implementing occlusion in the "SimulatedEnvironmentOcclusionSensor".

The sensor class also has properties 'pointVisibility' and 'objectVisibility', which store whether an point or object is visible for a time step. This is to model a depth camera sensor with a range and field of view, and occlusion caused by environment primitives. The base "SimulatedEnvironmentSensor" needs to run the 'setVisibility' method before generating measurements. This method checks the points for their visiblity in field of view of the camera for each time step and sets the values in 'pointVisibility', where the columns are points and rows are time steps. The "SimulatedEnvironmentOcclusionSensor" overloads the 'setVisibility' method to add occlusion implementation, and takes the environment it is constructed from as input. Occlusion is caused by the surfaces of rigid body primitives ("EP_Default" class instances with meshes), using the method outlined in section 4.4.

The sensor points and objects are finally used to generate a graph file consisting of measurements, through the 'generateMeasurements' method. It outputs two .graph format text files - a ground truth file consisting of the vertexes of the graph without any noise, and 'measurements' graph file that only has the edges of the graph. In the 'measurements' file, the vertex associations are provided as indexes but the vertices themselves are initialised by the graph class when the file is read to construct the SLAM factor graph. When 'generateMeasurements' is called it constructs the graph files by running the following process for every time step set in the 't' property of the config for the simulation:

1. Generate robot pose vertexes and odometry edges. Output the pose vertexes to ground truth graph file and the odometry edges to the measurements graph file.

2. Generate point observations from the robot sensor for the sensor points:

    2.1. Check whether the point is visible for the current time step and run the following steps if it's corresponding 'pointVisibility' entry is 1:

        2.1.1. If it is a static point, create a single vertex and store its value, unless the config property 'staticDataAssociation' is turned off, in which create a new vertex if the point was not observed in the previous time step. Create a measurement edge from the current time step robot pose to the most recent point vertex initialised in the measurements graph file.

        2.1.2. If it is a dynamic point, create a new vertex, and a measurement edge from the current time step robot pose vertex to the point vertex.

3. Generate point motion measurement according the config properties 'pointMotionMeasurement' and 'motionModel'. This is a switch case for each type of motion measurement or estimation described in section 4.5.

The sensor can also dynamically plot itself, with the sensor shown as a camera and visible points indicated in red, and unobserved points in black, with the same plotting styles as environment.

The .graph file text format contains lines where each line is a vertex or edge, identified by its corresponding label set in the config (for example, 'POSEVERTEX' for a robot pose or 'POSEPOSEEDGE' for robot odometry), value for that variable or measurement, and covariance upper triangular matrix.

5.2 DO-SLAM Back End

5.2.1 Graph

The graph class implements the factor graph by reading the graph file and creating instances of edge and vertex classes. Graphs are used to construct the solver system, and measure error between the ground truth graph and SLAM final estimate graph.

The "Vertex" class is generic for all types of vertices and has a property 'type' which distinguishes its type, for example 'pose', 'point' or 'motion'. It has a value and covariance for the Gaussian probability.

The "Edge" class is generic for all types of edges, however the 'type' property indicates what its input and output edges should be, which is used to select the correct Jacobian calculation function. "Edge" also has the 'covariance' which is the measurement error, and 'value' which is the value of its corresponding factor.

The graph is solved by running the 'process' method, which constructs the initial vertices of the factor graph from the measurements, forms the SLAM system consisting of Jacobian matrices and covariances, and conducts the non-linear least squares optimisation (explained in subsection 3.2.3). For every iteration of the SLAM solver, it computes the increment δ^* and updates the vertex and edge values in the graph, until the residual falls below the threshold set in config.

5.2.2 Solver

The SLAM solver is implemented by the "System" class and the "NonLinearSolver" class. The "System" class is the matrix representation of the "Graph" class factor graph. It constructs the information Jacobian matrix A by linearising the system based on the functions for graph edge type Jacobians, and the residuals vector $\mathbf{b}$ from the vertex prediction error values. The system is solved incrementally as mentioned in the previous section, using the method implementing the solution algorithm set in the config 'solverType' property. The correct operation of the motion measurements Graph and Solver is tested with the unit tests shown in section A.1.

5.3 Applications

An application a script of a full simulation of the environment with graph construction, solution and error calculation that tests our algorithms. The process followed in an application is as follows:

1. Setup a config with all of the labels, error settings, point motion model settings, filepaths, solver settings, camera parameters and other properties.
2. Instantiate an environment and add primitives and points to it by:
    2.1. Creating trajectories, and using the environment add functions to create ellipsoids, cubes or rectangles, OR
    2.2. Creating a set of points and adding them statically to the simulated environment.
3. Create a robot trajectory and sensor pose.

4. Instantiate a 'SimulatedEnvironmentSensor' or 'SimulatedEnvironmentOcclusionSensor' instance.
    4.1. Instantiate sensor objects and points from a simulated environment by running 'addEnvironment' with the environment as input.
    4.2. Set visibility for the points, if 'SimulatedEnvironmentOcclusionSensor' is used the environment is required as an input argument.
    4.3. (Optional) Animate a plot of the sensor over time to observe the visibility of points, and check the visibility of the points as set in 'pointVisibility'.
    4.4. Run 'generateMeasurement' to generate ground truth and measurements graph files.
    4.5. If the constant SE(3) motion vertex is used for point motion estimation, an additional function 'writeDataAssociationVerticesEdges' needs to be run to add the constructed motion vertex in the graph file.
5. Read the graph files as a cell array ('graphFileToCell' function).
6. Parse the cell array graph file into a Graph Class instance.
7. Run the 'solve' method on the graph to solve for the final SLAM estimate.
8. Save the solved results graph as a graph file using the 'saveGraphFile' method in Graph.
9. Run 'errorAnalysis' function with the ground truth and results graph as input to obtain accuracy values for the SLAM algorithm.
10. Plot the results and ground truth graph file ('plotGraph' or 'plotGraphFile' function).

An application can be run directly on the graph file by setting the appropriate labels in the "Config" following the process from step 6 onwards.

Chapter 6

Results

6.1 General Setup

Applications are created to test the solution accuracy of the different point motion measurement and estimation models (described in section 4.5) in the SLAM algorithm. Each application is a separate script with its own simulated environment meant to model a simplified version of a real world scenario, and multiple types of point motion measurements can be tested by repeating the simulation with different 'pointMotionMeasurement' and 'motionModel' settings (see subsection 5.1.1). All of the remaining config settings such as noise, solver and pose parametrisation are kept the same for all of the applications as summarised in Table 6.1.

The sensor noise is set based on realistic values for an abstract sensor that could theoretically create these types of motion measurements. High noise settings make the causes some of the solution estimates to move away from the local minimum for the NLS optimisation. Setting the point motion measurement noise very high in relation to the odometry ('stdPosePose') and camera sensor ('stdPosePoint') results in the motion measurement having negligible impact on the final estimate, whereas setting them too low causes the point trajectories to be become more innaccurate for applications where the linear point motion measurements are applied on non-linear motion as they cause a strong bias towards linear point motion trajectories.

Six measures of error are taken from the final SLAM estimate to observe the accuracy of the motion model in the solver. These are abbreviated in the tables of the results for every section in this chapter, and their full forms are explained here.

Absolute Trajectory Translation Error (ATE) The absolute (inertial frame) error in the translational component of the robot trajectory, in metres. It is a measure of how accurate the robot localisation with respect to th real or simulated.

Absolute Trajectory Rotation Error (ARE) The absolute (inertial frame) error in the rotational component of the robot trajectory, in degrees. It is another measure of how accurate the robot localisation is with respect to the real or simulated environment.

Table 6.1: Application config noise settings.

Label	**Error for**	**Set as**	**Value**
stdPosePrior	Prior for the sensor pose	0.01m position, 1 degree in euler axis of rotation.	[0.01, 0.01, 0.01, 0.0173, 0.0176, 0.0173]'
stdPosePose	Odometry/IMU	0.04m translation and 1 degree in each euler axis of rotation.	[0.04, 0.04, 0.04, 0.0173, 0.0176, 0.0173]'
stdPointPrior	Prior for initialising a point	0.01m position error in $\mathbb{R}^3$ (inertial frame)	[0.01, 0.01, 0.01]'
stdPosePoint	Point measurement error in sensor frame coordinates	0.04m position error in $\mathbb{R}^3$ (sensor frame)	[0.04, 0.04 0.04]'
stdPointPoint	2-point edge motion	0.01m translation in $\mathbb{R}^3$	[0.01, 0.01, 0.01]'
std3Points (speed)	3-point as a euclidean distance	0.01m distance translation	0.01
std3Points (velocity)	3-point motion as a translation vector	0.01m in $\mathbb{R}^3$	[0.01, 0.01, 0.01]'
std2PointsVelocity (speed)	Average speed motion model	0.01m euclidean distance	0.01
std2PointsVelocity (velocity)	Average velocity motion model	0.01m in $\mathbb{R}^3$	[0.01, 0.01, 0.01]'
std2PointsSE3Motion	Predicted motion position & actual	0.05m in $\mathbb{R}^3$	[0.05,0.05,0.05]'

Absolute Structure Points Error (ASE) The absolute position error of points in the environment, in metres. It is a measure of how accurate the map estimation is with respect to the actual environment.

All-to-All Relative Trajectory Translation Error (allRTE) The error in all of poses of the robot trajectory translational component with respect to each other, in metres. It is a measure of the accuracy of the SLAM algorithm in the robot's internal estimation of its trajectory, and informs us of the improvement in the SLAM localisation estimation from adding motion information.

All-to-All Relative Trajectory Rotation Error (allRRE) The error in all of poses of the robot trajectory rotational component with respect to each other, in degrees. It has the same purpose as allRTE.

All-to-All Relative Structure Points Error The error in the positions of the points with respect to each other, in metres. It is a measure of the consist-

ency of the robot's internal estimation of the environment and the spatial relationships between points within it, and informs us of the improvement in the SLAM map estimation from adding motion information.

6.2 Application 1: One Primitive Linear Motion

6.2.1 Application 1 Experimental Setup

This application tests the linear point motion models (2-point edge, 3-point edge, and velocity vertex) on an environment consisting of a single object with linear motion, thereby validating the use of these models and allowing for a comparison of their relative accuracy in solving a dynamic SLAM environment.

The simulation runs for 51 steps, set in simulated environment as 10 seconds. The motion of the primitive is set with equally spaced linear waypoints, and interpolated using a straight line fit, starting with an initial position of $[20, 0, 0]$ with an inertial frame waypoints $[2.5, 1, 0.5]m$ apart per second. The robot tracks behind it with a linear interpolated trajectory also set with waypoints. The plot for this environment is shown in Figure 6.1. This application demonstrates the accuracy of the point motion measurement types on a valid environment motion model, thereby allowing us to directly compare their performance in improving the SLAM estimate.

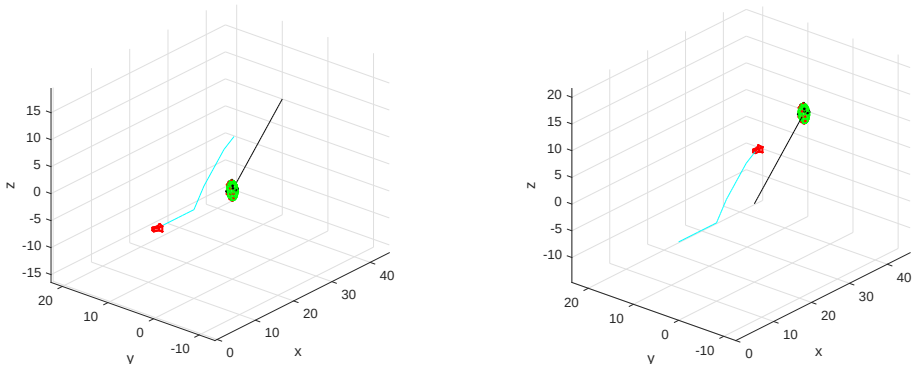

(a) Step 1 (b) Step 51

Figure 6.1: Application 1: One Primitive Linear Motion Environment simulated environment sensor plots. Red points are visible in the sensor, black points are not.

6.2.2 Application 1 Results

Four observations can be made from the results shown in Figure 6.2 and Table 6.2. 1) The velocity motion model (vector) measurements are more accurate than the speed measurements for the 3-point edge, but less accurate for the velocity vertex. 2) The

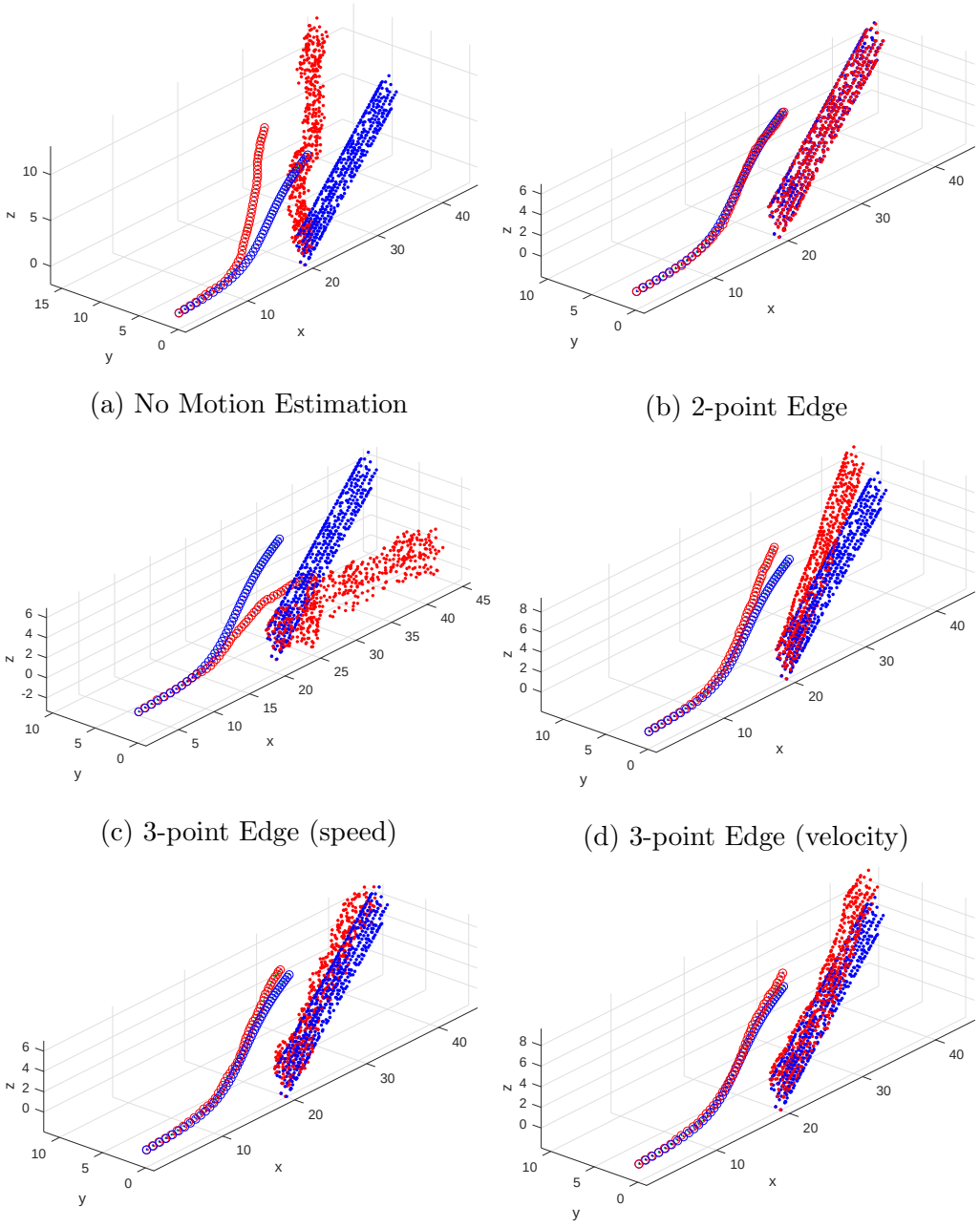

(a) No Motion Estimation

(b) 2-point Edge

(c) 3-point Edge (speed)

(d) 3-point Edge (velocity)

(e) Velocity Vertex (speed)

(f) Velocity Vertex (velocity)

Figure 6.2: Application 1: One Primitive Linear Motion Results. Red is SLAM solver final estimate and blue is ground truth. Circles with axes in them are robot poses and dots are point positions.

most accurate solution is done by the 2-point edge, however it is also an unrealistic model as in a real world sensor such measurements are difficult to collect. 3) The velocity vertex is more accurate than the 3-point edge for pure linear motion. 4) Implementing the linear motion model measurements increases the point position estimate accuracy at the expense of increased error in the robot trajectory.

Table 6.2: Application 1 Results

Test	**ATE (m)**	**ARE (°)**	**ASE (m)**	**allRTE (m)**	**allRRE (°)**	**allRSE (m×10^{-3})**
No motion edges	2.008	11.002	0.854	0.019	0.173	2.481
2-point edge	0.185	1.793	0.062	0.005	0.043	0.186
3-point edge (speed)	1.585	10.937	0.742	0.018	0.156	2.137
3-point edge (velocity)	0.635	5.279	0.188	0.008	0.078	0.543
Velocity vertex (speed)	0.485	3.774	0.486	0.008	0.076	1.415
Velocity vertex (velocity)	0.543	3.800	0.353	0.011	0.074	1.041

6.3 Application 2: Two Primitives Non-Linear Motion

6.3.1 Application 2 Experimental Setup

We now test the effectiveness of the linear point motion measurements outside their valid domain, i.e. for cases where the motion of the points is non-linear and includes both translational and rotational components. Application 2 contains two moving primitives, each with non-linear motion set through waypoints.

The waypoints are written here in MATLAB format with semicolons indicating rows: the first row contains the time values, second row corresponding x values, third row y values and fourth row z values. Primitive 1 waypoints are [0:2:10; 10, 20, 30, 35, 40 41; 0, 3, 5, -3, -5, -5; 0, 0, 0, 0, 0, 0] and Primitive 2 waypoints are [0:2:10; 15, 20, 25, 27, 30, 35; -2, -4, -2, 0, 0, 1; 1, 0, 0, 1, 0.5, 0].

In total both primitives have 52 environment points that are sensed by the robot. The simulation is run for 51 steps (10 seconds). The plots for step 1 and step 51 are shown in Figure 6.3.

6.3.2 Application 2 Results

As shown in Figure 6.4 and Table 6.4, for the limited number of steps in this simulation, the error in the SLAM estimate does not increase drastically when a linear motion model is applied to estimate non-linear point motion, as the time step size is small (0.2s) and the relative motion between two time steps is small for each point.

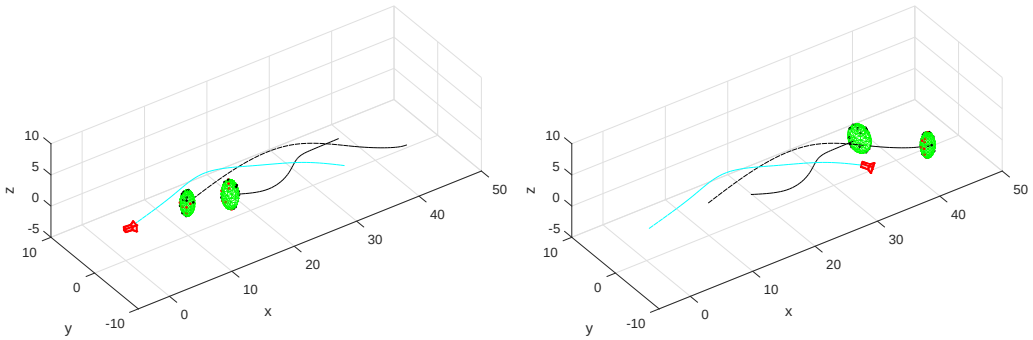

(a) Step 1 (b) Step 51

Figure 6.3: Application 2: Two Primitives Non-Linear Motion Environment simulated environment sensor plots. Red points are visible in the sensor, black points are not.

Table 6.3: Application 2 Results

Test	**ATE (m)**	**ARE (°)**	**ASE (m)**	**allRTE (m)**	**allRRE (°)**	**allRSE (m×10^{-3})**
No motion edges	2.039	11.111	0.949	0.021	0.175	1.985
2-point edge	0.278	1.907	0.203	0.006	0.042	0.429
3-point edge (speed)	0.535	4.964	0.848	0.017	0.123	1.805
3-point edge (velocity)	1.090	5.836	0.390	0.010	0.089	0.837
Velocity vertex (speed)	0.657	8.170	0.455	0.010	0.093	0.996
Velocity vertex (velocity)	0.668	4.215	0.334	0.011	0.073	0.701

In this application, the speed motion models perform better than the velocity models for both the robot trajectory and map estimate. One reason for this could be the relative flexibility in the constraint implemented that makes no assumption on the direction of motion for the point.

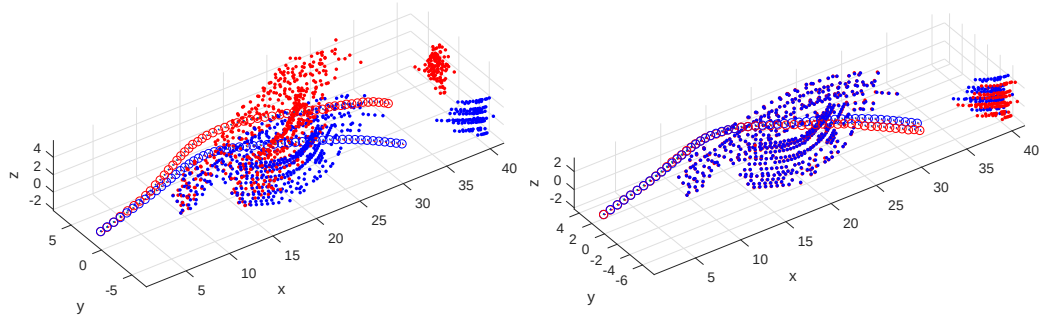

(a) No Motion Estimation

(b) 2-point Edge

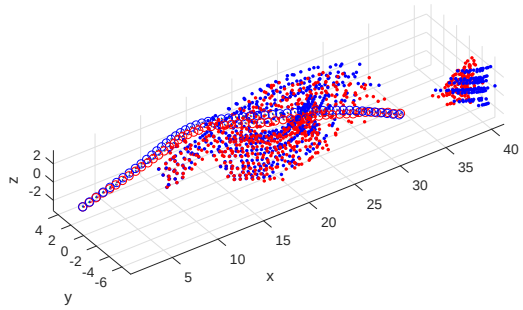

(c) 3-point Edge (speed)

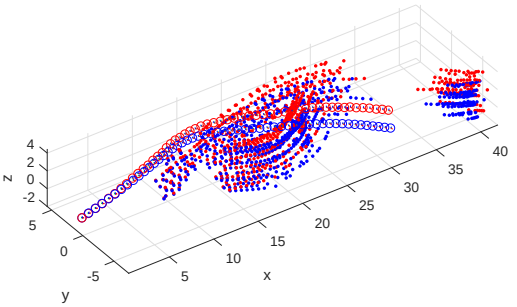

(d) 3-point Edge (velocity)

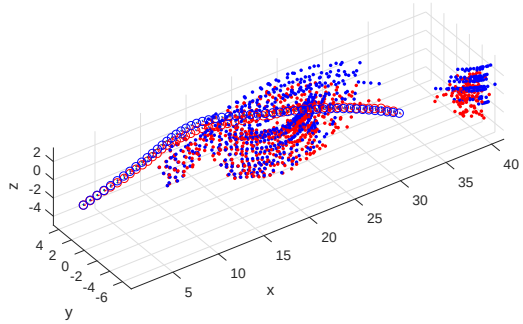

(e) Velocity Vertex (speed)

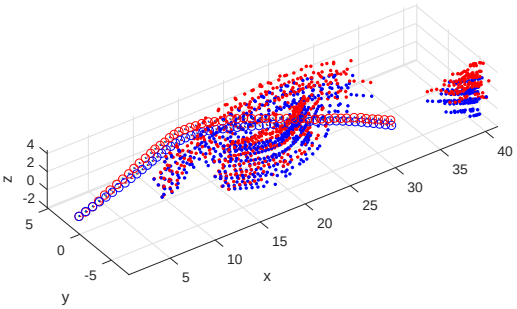

(f) Velocity Vertex (velocity)

Figure 6.4: Application 2: Two Primitives Non-Linear Motion Results. Red is SLAM solver final estimate and blue is ground truth. Circles with axes in them are robot poses and dots are point positions.

6.4 Application 3: One Primitive Non-Linear Motion + Static Points

6.4.1 Application 3 Experimental Setup

We expand the case in section 6.3 to include static points in the scene, that are repeatedly observed from multiple robot posts in conjuntion with the dynamic points

and their motion on the primitive. SLAM research literature shows that loop-closure improves the SLAM estimation[13]. There are 126 points in this simulation, 100 static and 26 dynamic. Static points are initialised along planes modelling walls, behind the primitive so that occlusion occurs. Primitive waypoints are set as (using MATLAB notation as explained in subsection 6.3.1): [0:2:10; 10, 20, 25, 20, 10, 5; 0, 0, 10, 15, 15, 15; 0, 2, 1, 3, ,5 2]. The simulation is run for 51 time steps (simulation time 10s). The plot of the environment at step 1 and 51 is in Figure 6.5.

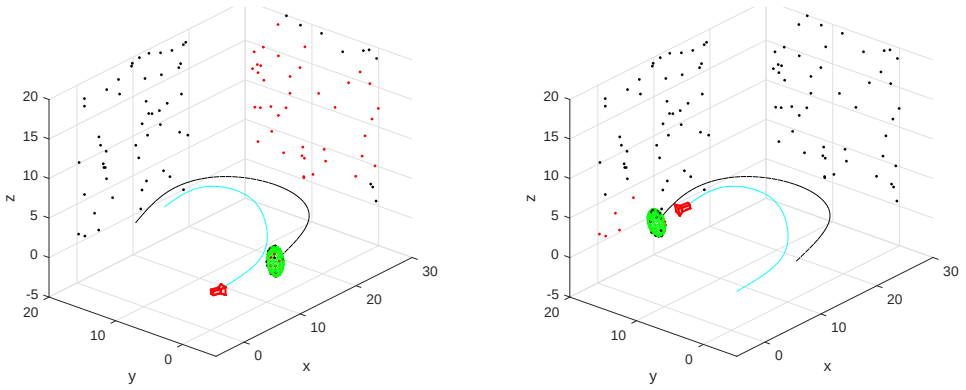

(a) Step 1 (b) Step 51

Figure 6.5: Application 1: Two Primitives Non-Linear Motion Environment simulated environment sensor plots. Red points are visible in the sensor, black points are not.

6.4.2 Application 3 Results

The results in Table 6.4 and Figure 6.6 illustrate that loop-closure from repeated observation of static points increases the overall SLAM estimation accuracy. However, applying a linear motion model to non-linear motion can worsen the accuracy of the SLAM estimate compared to if the system is optimised using repeat measurements of static points alone, particularly for the 3-point edge and velocity vertex scalar measurements. The 3-point edge (velocity) is the only measure that improves SLAM estimate for both robot trajectory and point positions, however the exact reason is difficult to determine.

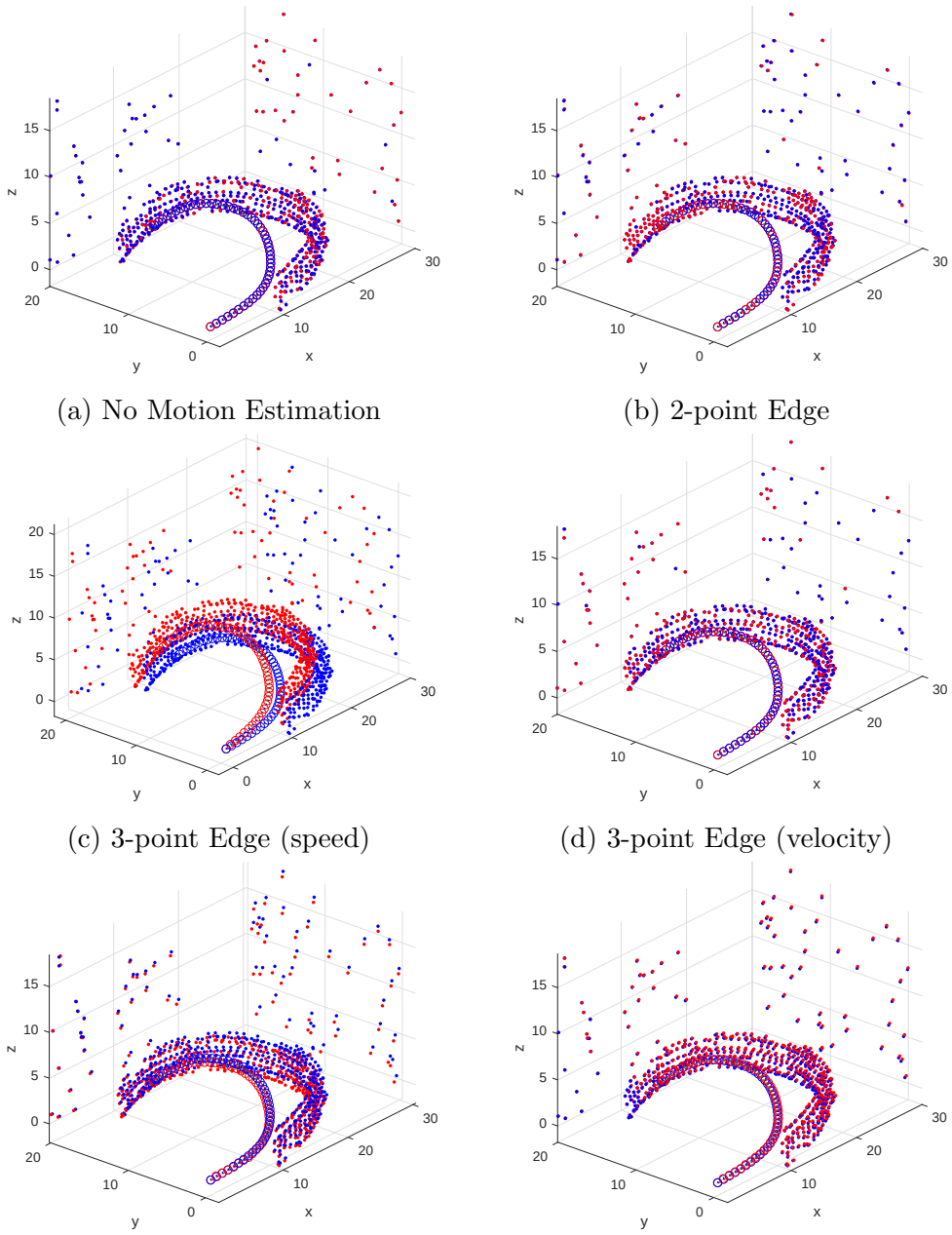

(a) No Motion Estimation

(b) 2-point Edge

(c) 3-point Edge (speed)

(d) 3-point Edge (velocity)

(e) Velocity Vertex (speed)

(f) Velocity Vertex (velocity)

Figure 6.6: Application 3: One Primitive Non-Linear Motion + Static Points Results. Red is SLAM solver final estimate and blue is ground truth. Circles with axes in them are robot poses and dots are point positions. Note subfigure (c) where the SLAM estimate is noticeably made worse.

Table 6.4: Application 3 Results

Test	**ATE (m)**	**ARE (°)**	**ASE (m)**	**allRTE (m)**	**allRRE (°)**	**allRSE (m×10^{-3})**
No motion edges	0.046	0.240	0.061	0.001	0.005	0.164
2-point edge	0.049	0.427	0.036	0.001	0.005	0.098
3-point edge (speed)	3.813	14.428	0.079	0.029	0.144	0.216
3-point edge (velocity)	0.026	0.177	0.061	0.001	0.005	0.164
Velocity vertex (speed)	0.657	8.170	0.455	0.010	0.093	0.996
Velocity vertex (velocity)	0.275	1.130	0.057	0.002	0.015	0.155

6.5 Applications 4 and 5: Constant Motion Primitives

Applications 4 and 5 test the constant motion vertex, which is the most general motion model and can estimate the point translation and rotation for the points associated to an object, provided it is constant for the entire simulation. The environments in these applications model primitives with constant motion trajectories and test the accuracy of the SLAM estimate with incorporation of the constant motion. This is an estimation, where the motion vertex is initialised from the point measurements by finding the inertial frame relative transform (4.32).

6.5.1 Application 4: Two Primitives Constant Motion Experimental Setup

In Application 4, the robot follows a figure of 8 trajectory in between 2 objects that follow a circular trajectory, and observes points on the objects at various times. The simulation is run for 120 seconds with 121 time steps. In Figure 6.7, primitive 1 (left) has a $\mathfrak{se}(3)$ constant motion of u_1 = [1.2226, 1.4476, 0, 0, 0, 0.105], and primitive 2 (right) has a constant motion of u_2 = [-1.2226, 1.4476, 0, 0, 0, -0.105]. The total number of points from both ellipsoids is 22.

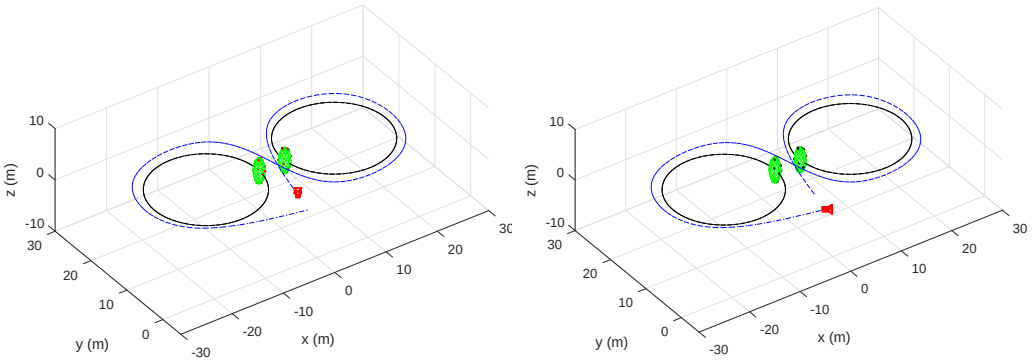

(a) Step 1 (b) Step 121

Figure 6.7: Application 4: Two Primitives Constant Motion Environment simulated environment sensor plots. Red points are visible in the sensor, black points are not.

6.5.2 Application 5: One Primitive Constant Motion + Static Points Experimental Setup

In Application 5, the environment consists of an object moving in a screw trajectory in front of static points created along rectangles. The primitive has a $\mathfrak{se}(3)$ motion transform of u = [0.9938, -0.4028, -0.0013, 0.001, 0.0002, 0.06]. There are static points and dynamic points in the environment. This simulation is also from t=0s to t=120s with 121 time steps. Robot motion is set via waypoints tracking behind the primitive. The plot for the environment is shown in Figure 6.8.

Application 5 is tested with and without loop closure. With loop closure, static points in the environment are observed in the first and final time steps and associated together. Without loop closure, the static points are not associated and new vertices are created when the same point is observed again after losing track in the robot sensor.

6.5.3 Application 4 and 5 Results

From Figures Figure 6.9 and Figure 6.10, and Table 6.5 it can be seen that implementing the constant motion estimation of points in an environment, where the motion model is valid, improves the general accuracy of the environment map. However, often there is a tradeoff between improving the map estimate and a less accurate robot trajectory estimate.

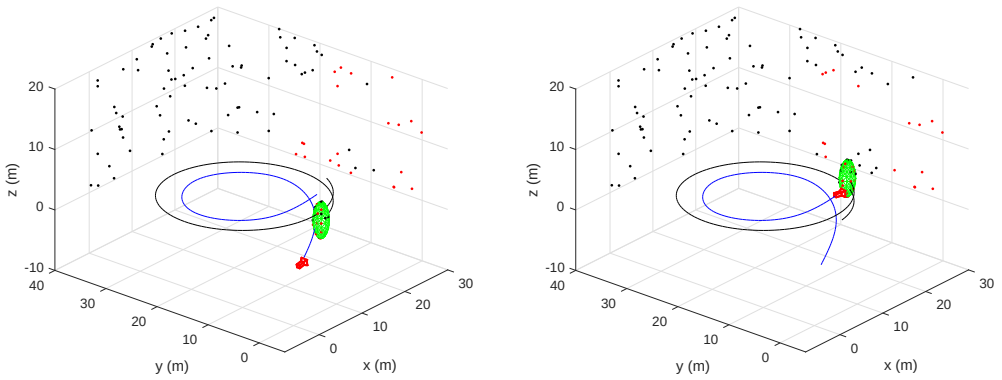

(a) Step 1 (b) Step 121

Figure 6.8: Application 5: One Primitive Constant Motion + Static Points simulated environment sensor plots. Red points are visible in the sensor, black points are not.

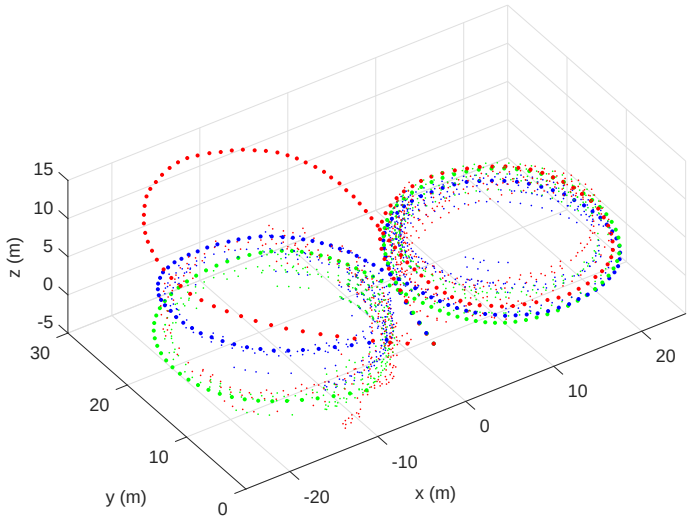

Figure 6.9: Application 4 solver results. Large dots represent robot positions and small dots point locations. Green colour denotes ground truth, blue denotes SLAM solution with the SE(3) transform and red denotes the SLAM solution without the SE(3) transform.

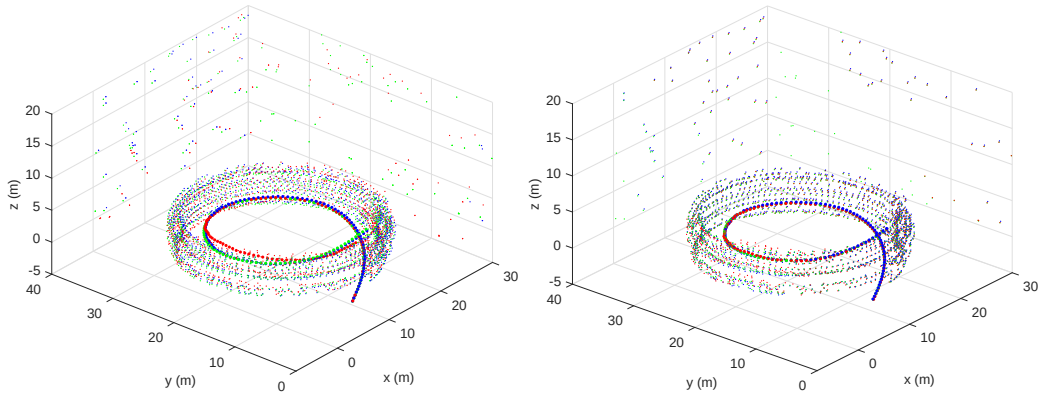

(a) Without Loop Closure (b) With Loop Closure

Figure 6.10: Application 5 solver results. Large dots represent robot positions and small dots point locations. Green colour denotes ground truth, blue denotes SLAM solution with the SE(3) transform and red denotes the SLAM solution without the SE(3) transform.

Table 6.5: Application 4 and 5 Results 'a' and 'b' indicate the application results with and without without application of the constant motion vertex respectively. 'wolc' means without loop closure, 'wlc' means with loop closure.

Application Setup	**ATE (m)**	**ARE (°)**	**ASE (m)**	**allRTE (m)**	**allRRE (°)**	**allRSE (m$\times 10^{-3}$)**
4-a	5.442	15.625	1.968	0.019	0.099	4.076
4-b	2.282	7.566	0.650	0.009	0.035	1.442
5-wolc-a	0.592	5.228	1.234	0.008	0.056	1.091
5-wolc-b	0.428	1.651	0.126	0.002	0.010	0.113
5-wlc-a	0.100	0.937	0.163	0.002	0.013	0.170
5-wlc-b	0.195	1.232	0.074	0.001	0.007	0.072

Chapter 7

Conclusion

The goal of this honours thesis is to conceptualise and develop the front-end of the DO-SLAM Framework (chapter 5), and use it to test the validity and accuracy of different motion measurement and estimations models that are integrated in a SLAM algorithm. I evaluate the performance of six theoretical motion measurement and estimation models (section 4.5), which are tested on simulated data.

I also describe the Dynamic Object SLAM (DO-SLAM) framework which is the broader subject of the research program I am a part of. DO-SLAM incorporates methods of adding the structure [5] and motion [2] of objects in the environment in order to improve the SLAM estimation. My contributions to this research program include helping conceptualise the overall structure of the framework (section 4.1), adding the functionality to create primitives with abstract surface representations (subsection 5.1.4), designing and implementing occlusion (section 4.4) in the abstract simulated environment sensors, adding functionality to create graph files with point motion measurements and constraints, and testing of the algorithms on simulated data (chapter 6).

From the results in chapter 6, we can see that in general adding more information to the SLAM system for dynamic environments improves the SLAM estimate accuracy, in particular for environments with only dynamic objects. However, the improvement to the map and robot trajectory estimate is decreased in cases where the solution motion model is not valid for the actual motion of the corresponding points in the environment. The measurements created according to linear point motion models are not robust in cases where they the object motion is actually non-linear, and in some cases reduces the accuracy of the SLAM estimate, particularly when used in conjunction with the conventional static point tracking and loop closure methods (see sections section 6.2 and section 6.4).

The constant motion vertex is an improvement on the linear point motion assumptions as it uses the SE(3) transformation of the object in the inertial frame, and is the most generalised which results in consistent improvement in the SLAM estimation when applied to points and objects where it is a valid model, as evidenced in subsection 6.5.3. Furthermore, through deriving geometric relationships we

show that the constant motion transform in the inertial frame for a set of grouped points moving in a 3D environment can be derived without explicitly requiring their geometric relationship with their associated object (subsection 4.5.4), which expands the application potential of this method. As it is an estimation that provides a structure to the already existing point measurements from the robot sensor, it is applicable to a real-world environment in comparison to the linear point motion models which all assume that there independent measurements of the point's motion or average velocity can be obtained.

To further develop this concept, the constant motion assumption needs to be further developed as a derivation or in implementation to make it robust and applicable in a real world environment. Segmenting the motion of a group of points by time step and applying the constant motion assumption for a set of time steps instead of the entire observation time is one possible method of doing this. Furthermore, we assume that the data association problem is solved in the simulated environment, however in the real world data association is a significant task and additional techniques such as CNN based image recognition will need to be integrated on camera sensor data to data associate and track objects. The current developed algorithms also require a rigid body assumption to be a valid model the object, which needs to be adapted further to operate with real world deformable bodies such as pedestrians that commonly form part of a dynamic environment.

Appendix 1

A.1 Unit Tests

The correct implementation of the point motion model in the solver algorithm is demonstrated by unit tests, where we manually construct a simple system of 3 points moving over 3 time steps with a robot observing it, without using the front-end of the framework. The motion of the points is set to be linear for the 2-point edge, 3-point edge and velocity vertex motion measurements to test cases where the algorithm's motion model is valid.

The points are initialised as part of an object in the object frame. The constant motion is applied to the object, and the point positions are found in the inertial frame to construct the sensor measurement edges and motion measurement edges/vertices. Error settings are in Table A.1 and results for all of the unit tests are in Table A.2, where the error measures have been explained in section section 6.1. Figures A.2 and A.1 show the visual plot of the results.

Table A.1: Unit test config noise settings

Label	**Measure**	**Set as**	**Value**
stdPosePrior	Prior for the sensor pose error	0.005m translation, 1 degree error in each Axis-Angle dimension.	[0.0050, 0.0050, 0.0050, 0.0175, 0.0175, 0.0175]
stdPosePose	Odometry/IMU pose change error	0.04m translation and 2 degree in each Axis-Angle dimension.	[0.0400, 0.0400, 0.0400, 0.0873, 0.0873, 0.0873]
stdPointPrior	Prior for initialising a point based on measurements	0.01m position error in R3 (inertial frame)	[0.01, 0.01, 0.01]
stdPosePoint	Point measurement error in sensor frame coordinates	0.04m position error in $\mathbb{R}^3$ (sensor frame)	[0.04, 0.04 0.04]

Table A.2: Unit test Results

Test	**ATE (m)**	**ARE (°)**	**ASE (m)**	**allRTE (m)**	**allRRE (°)**	**allRSE ($\mathbf{m}\times10^{-3}$)**
No motion edges	0.206	2.507	0.778	0.116	1.254	147.086
2-point edge	0.245	3.015	0.260	0.132	1.489	46.009
3-point edge (scalar)	0.169	2.932	0.741	0.086	1.443	139.250
3-point edge (vector)	0.169	2.924	0.411	0.081	1.455	78.293
Velocity vertex (scalar)	0.154	2.918	0.796	0.081	1.454	147.391
Velocity vertex (vector)	0.177	2.838	0.411	0.085	1.409	77.127
Constant Motion Vertex	0.233	2.174	0.634	0.113	1.087	114.749

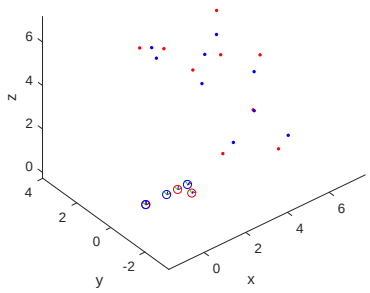

Figure A.1: Unit Test Results for the constant motion vertex explained in subsection 4.5.4. The motion input includes both translation and rotation. Red is final solution estimate and blue is ground truth. Circles with axes are robot poses and dots are point positions.

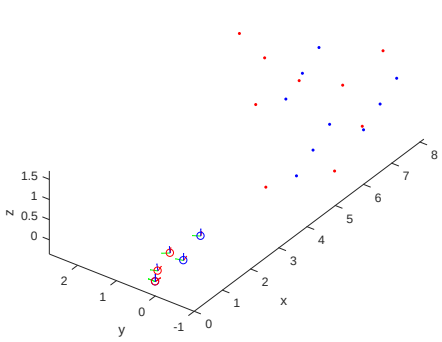

(a) No motion measurements

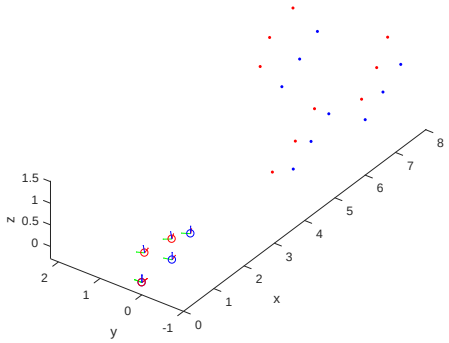

(b) 2-Point Edge

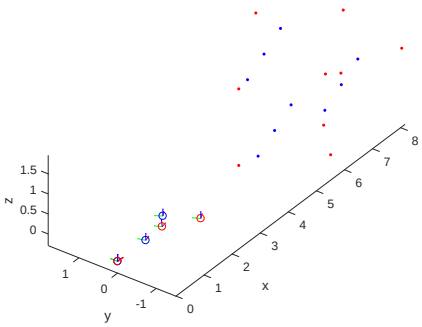

(c) 3-Point Edge (speed)

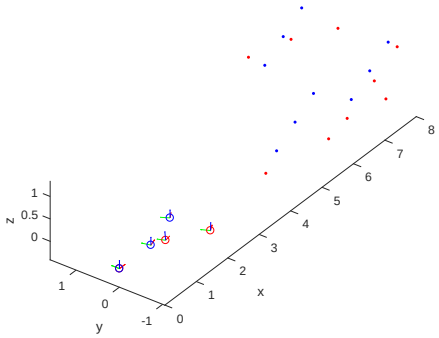

(d) 3-Point Edge (velocity)

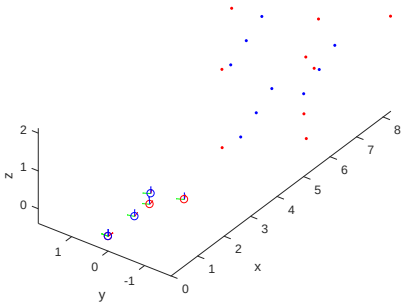

(e) Velocity Vertex (speed)

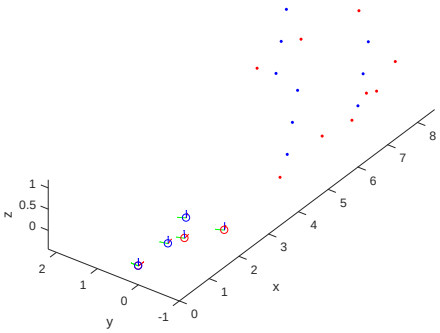

(f) Velocity Vertex (velocity)

Figure A.2: Unit Test Results for all of the linear point motion models implemented in the solver. Red is final solution estimate and blue is ground truth. Circles with axes are robot poses and dots are point positions.

Bibliography

[1] "MathWorks transform cartesian coordinates to spherical - cart2sph," https://au.mathworks.com/help/matlab/ref/cart2sph.html, accessed: 2017-10-21.

[2] M. Henein, Y. Vyas, J. Trumpf, V. Ila, and R. Mahony, "Simultaneous localization, mapping and tracking in dynamic environments," in *2018 IEEE International Conference on Robotics and Automation*. Institute of Electrical and Electronics Engineers (IEEE), 2018, submission.

[3] H. Durrant-Whyte and T. Bailey, "Simultaneous localization and mapping: part i," *IEEE Robotics Automation Magazine*, vol. 13, no. 2, pp. 99–110, June 2006.

[4] F. Dellaert and M. Kaess, "Square root SAM: Simultaneous localization and mapping via square root information smoothing," *The International Journal of Robotics Research*, vol. 25, no. 12, pp. 1181–1203, dec 2006.

[5] M. Henein, M. Abello, V. Ila, and R. Mahony, "Exploring the effect of meta-structural information on the global consistency of slam," in *2017 IEEE/RSJ International Conference on Intelligent Robots and Systems*, 2017.

[6] A. Cunningham, V. Indelman, and F. Dellaert, "DDF-SAM 2.0: Consistent distributed smoothing and mapping," in *2013 IEEE International Conference on Robotics and Automation*. Institute of Electrical and Electronics Engineers (IEEE), may 2013.

[7] A. Cunningham, K. M. Wurm, W. Burgard, and F. Dellaert, "Fully distributed scalable smoothing and mapping with robust multi-robot data association," in *2012 IEEE International Conference on Robotics and Automation*. Institute of Electrical and Electronics Engineers (IEEE), may 2012.

[8] R. F. Salas-Moreno, R. A. Newcombe, H. Strasdat, P. H. Kelly, and A. J. Davison, "SLAM++: Simultaneous localisation and mapping at the level of objects," in *2013 IEEE Conference on Computer Vision and Pattern Recognition*. Institute of Electrical and Electronics Engineers (IEEE), jun 2013.

[9] A. Walcott-Bryant, M. Kaess, H. Johannsson, and J. J. Leonard, "Dynamic pose graph SLAM: Long-term mapping in low dynamic environments," in *2012*

IEEE/RSJ International Conference on Intelligent Robots and Systems. Institute of Electrical and Electronics Engineers (IEEE), oct 2012.

[10] C. Bibby and I. Reid, "Simultaneous localisation and mapping in dynamic environments (slamide) with reversible data association," in *Proceedings of Robotics Science and Systems*, vol. 117, 2007, p. 118.

[11] C.-C. Wang, C. Thorpe, S. Thrun, M. Hebert, and H. Durrant-Whyte, "Simultaneous localization, mapping and moving object tracking," *The International Journal of Robotics Research*, vol. 26, no. 9, pp. 889–916, 2007. [Online]. Available: https://doi.org/10.1177/0278364907081229

[12] J.-L. Blanco, "A tutorial on se(3) transformation parameterizations and on-manifold optimization," Universidad de Malaga, Tech. Rep., 2014.

[13] J. Engel, V. Koltun, and D. Cremers, "Direct sparse odometry," *ArXiv e-prints*, Jul. 2016.